A peer-reviewed version of this preprint was published in PeerJ on 10 January 2019.

View the peer-reviewed version (peerj.com/articles/6190), which is the preferred citable publication unless you specifically need to cite this preprint.

Pfeifer M, Boyle MJW, Dunning S, Olivier PI. 2019. Forest floor temperature and greenness link significantly to canopy attributes in South Africa's fragmented coastal forests. PeerJ 7:e6190
https://doi.org/10.7717/peerj.6190

Forest floor temperature and greenness link significantly to canopy attributes in South Africa's fragmented coastal forests

Marion Pfeifer Corresp., [1] , **Michael JW Boyle** [2] , **Stuart Dunning** [3] , **Pieter Olivier** [4]

[1] School of Natural and Environmental Sciences, University of Newcastle-upon-Tyne, Newcastle Upon Tyne, United Kingdom
[2] Department of Life Sciences, Imperial College London, Ascot, Berkshire, United Kingdom
[3] School of Geography, Politics and Sociology, University of Newcastle-upon-Tyne, Newcastle Upon Tyne, United Kingdom
[4] M.A.P. Scientific Services, Pretoria, South Africa

Corresponding Author: Marion Pfeifer
Email address: marion.pfeifer@ncl.ac.uk

Tropical landscapes are changing rapidly due to changes in land use and land management. Being able to predict and monitor land use change impacts on species for conservation or food security concerns requires the use of habitat quality metrics, that are consistent, can be mapped using above - ground sensor data and are relevant for species performance. Here, we focus on ground surface temperature ($Thermal_{ground}$) and ground vegetation greenness ($NDVI_{down}$) as potentially suitable metrics of habitat quality. We measure both across habitats differing in tree cover (natural grassland to forest edges to forests and tree plantations) in the human-modified coastal forested landscapes of Kwa-Zulua Natal, South Africa. We show that both habitat quality metrics decline linearly as a function of increasing canopy closure (*FCover*, %) and canopy leaf area index (*LAI*). Opening canopies by about 20% or reducing canopy leaf area by 1% would result in an increase of temperatures on the ground by more than 1°C, and an increase in ground vegetation greenness by 0.2 and 0.14 respectively. Upscaling *LAI* and *FCover* to develop maps from Landsat imagery using random forest models allowed us to map $Thermal_{ground}$ and $NDVI_{down}$ using the linear relationships. However, map accuracy was constrained by the predictive capacity of the random forest models predicting canopy attributes and the linear models linking canopy attributes to the habitat quality metrics. Accounting for micro-scale variation in temperature is seen as essential to improve biodiversity impact predictions. Our upscaling approach suggests that mapping ground surface temperature based on radiation and vegetation properties might be possible, and that canopy cover maps could provide a useful tool for mapping habitat quality metrics that matter to species. However, we need to increase sampling of surface temperature spatially and temporally to improve and validate upscaled models. We also need to link surface temperature maps to demographic traits of species of different threat status or functions in landscapes with different disturbance and management histories testing for generalities

in relationships. The derived understanding could then be exploited for targeted landscape restoration that benefits biodiversity conservation and food security sustainably at the landscape scale.

Forest floor temperature and greenness link significantly to canopy attributes in South Africa's fragmented coastal forests

Pfeifer M[a,*], Boyle MJW[b], Dunning S[c], Olivier P[d]

[a] Modelling, Evidence & Policy Group, SNES, Newcastle University, Newcastle Upon Tyne, NE7 1RU, UK. Email: marion.pfeifer@newcastle.ac.uk.

[b] Forest Ecology and Conservation Group, Imperial College London, Silwood Park Campus, Buckhurst Road, Ascot, Berks, SL5 7PY, UK. Email: michael.boyle11@imperial.ac.uk

[c] School of Geography, Politics and Sociology, Newcastle University, Newcastle Upon Tyne, NE7 1RU, UK. Email: stuart.dunning@ncl.ac.uk

[d] M.A.P. Scientific Services, Pretoria, South Africa. Email: pieter.i.olivier@gmail.com

* Corresponding author: marion.pfeifer@newcastle.ac.uk, +44 7732327961

Abstract

Tropical landscapes are changing rapidly due to changes in land use and land management. Being able to predict and monitor land use change impacts on species for conservation or food security concerns requires the use of habitat quality metrics, that are consistent, can be mapped using above - ground sensor data and are relevant for species performance. Here, we focus on ground surface temperature ($Thermal_{ground}$) and ground vegetation greenness ($NDVI_{down}$) as potentially suitable metrics of habitat quality. We measure both across habitats differing in tree cover (natural grassland to forest edges to forests and tree plantations) in the human-modified coastal forested landscapes of Kwa-Zulua Natal, South Africa. We show that both habitat quality metrics decline linearly as a function of increasing canopy closure (*FCover*, %) and canopy leaf area index (*LAI*). Opening canopies by about 20% or reducing canopy leaf area by 1% would result in an increase of temperatures on the ground by more than 1°C, and an increase in ground vegetation greenness by 0.2 and 0.14 respectively. Upscaling *LAI* and *FCover* to develop maps from Landsat imagery using

random forest models allowed us to map $Thermal_{ground}$ and $NDVI_{down}$ using the linear relationships. However, map accuracy was constrained by the predictive capacity of the random forest models predicting canopy attributes and the linear models linking canopy attributes to the habitat quality metrics. Accounting for micro-scale variation in temperature is seen as essential to improve biodiversity impact predictions. Our upscaling approach suggests that mapping ground surface temperature based on radiation and vegetation properties might be possible, and that canopy cover maps could provide a useful tool for mapping habitat quality metrics that matter to species. However, we need to increase sampling of surface temperature spatially and temporally to improve and validate upscaled models. We also need to link surface temperature maps to demographic traits of species of different threat status or functions in landscapes with different disturbance and management histories testing for generalities in relationships. The derived understanding could then be exploited for targeted landscape restoration that benefits biodiversity conservation and food security sustainably at the landscape scale.

Highlights

- Ground surface temperatures and vegetation greenness vary between habitat types.
- Both decline linearly with increasing canopy closure (*FCover)* and leaf area *(LAI)*.
- For *FCover* increasing by 10%, temperature declined by 0.6°C and greenness by 0.1.
- For LAI increasing by 1 unit, temperature declined by 1°C and greenness by 0.14.
- Upscaling temperature and greenness is constrained by canopy attributes' maps.

Keywords

coastal forests, human-modified tropical landscapes, microclimate, habitat heterogeneity, mapping microclimate

1. Introduction

In increasing parts of the tropics, landscapes are experiencing anthropogenic loss and degradation of natural habitats, including primary forests, woodlands, and grasslands. The outcomes are landscape mosaics that comprise patches of natural habitat and regrowth, tree plantations and croplands of differing extents and management intensities. The subsequent erosion of biodiversity in these landscapes (Gibson et al., 2011) is an important global challenge for biodiversity conservation as well as climate change mitigation and food securities (Godfray et al., 2010). Natural habitats deliver carbon storage, hydrology and microclimate regulation services and supply resources used in construction, energy generation and trade. They typically harbour more species (Gibson et al., 2011) and more threatened species (Pfeifer et al., 2017) compared to plantations or croplands.

However, the fate of individual species following land use and management changes are difficult to predict. This is partly because we lack knowledge on species' habitat and resource needs at landscape scales in particular in the tropics, many models ignore that species perceive landscapes as continuous gradients in habitat quality rather than habitat categories (but see (Pfeifer et al., 2017), and we lack common indicators characterising habitat quality, which has been measured through various attributes or impacts on species' demographic traits (Chaplin-Kramer et al., 2015). Calls for standardised landscape metrics describing continuous variations in habitat quality at the landscape scale are increasing (Mortelliti, Amori & Boitani, 2010; Pfeifer et al., 2017) to fill that knowledge gap. And remote sensing has been advocated in the biodiversity literature as an ideal tool to obtain such metrics (Pettorelli et al., 2016), providing land surface data that are consistent, borderless, global and can be repeated across time. However, existing remote sensing derived metrics tend to focus on biomass or canopy vegetation productivity, which show inconclusive relationships with habitat attributes that matter to species.

Microclimate, and in particular thermal environment, has been suggested as a main driver for species community structure, affecting individual species and their interactions (Rae et al., 2006; Hemmings & Andrew, 2017). Temperature is a key driver for the growth, survival, and abundance of insects (Bale et al., 2002). Temperature can control community composition and diversity with examples showing shifts in the abundance of insect species tracking fluctuations in ground surface temperature within and across habitats

(Retana & Cerdá, 2000). Altitudinal migration among tropical bird (Barçante, M. Vale & Maria, 2017) and bat (Mcguire & Boyle, 2013) communities is little understood, but temporal availability of food resources (in particular insects) and direct impact of climate on physiological challenges to survival are among the key hypothesised drivers (Mcguire & Boyle, 2013). The productivity of the ground vegetation, which in forested stands constitutes the herbaceous layer, is also likely to play an important ecological role for species (Gilliam, 2007). The ground layer mediates nutrient fluxes, produces short-lived aboveground biomass and provides resources to ground-dwelling organisms (Bromham et al., 1999; Stork and Grimbacher, 2006)

Forest canopy structure can be up-scaled and mapped using remote sensing data (Hadi et al., 2017; Pfeifer et al., 2012, 2016). Expected relationships with temperature (Hardwick et al., 2015; Von Arx et al., 2012) as well as vegetation productivity on the ground (Royo et al., 2010; Shirima et al., 2015) may provide a potential approach to map and monitor temperature and vegetation growth as important microhabitat metrics on the forest floor. Vegetation cover insulates against temperature extremes and macroclimatic changes (Suggitt et al., 2011). Vegetation structure changes are expected to underlie temperature changes along gradients of forest degradation (Blonder et al., 2018), along forest edges (Didham & Lawton, 1999; Ewers & Banks-Leite, 2013), and with forest conversion to other land uses (Hardwick et al., 2015; Meijide et al., 2018). Ground vegetation growth and microclimate are likely to be interlinked, with vegetation acting as heat and water reservoir reducing soil evaporation and altering wind flow and vertical vapor transfer (Matthews, 2005).

A key challenge for this potential upscaling approach is to test whether general rules exist linking vegetation canopy structure to changes in $Thermal_{ground}$ and $NDVI_{down}$. Here, we focus on $Thermal_{ground}$ and $NDVI_{down}$ as indicators of habitat quality in coastal human-modified landscapes of Kwa-Zulu Natal, South Africa. We test for habitat quality variation along gradients of tree cover from 0 (grassland) to > 50% (natural coastal forests) and measure across edges separating forests from grasslands and forests from *Eucalyptus* plantations. We ask two main questions: (1) Are both descriptors of habitat quality variation interlinked?, and (2) Can we statistically link continuous changes in $Thermal_{ground}$ and $NDVI_{down}$ to

continuous changes in percentage canopy closure (*FCover*), canopy leaf area index (*LAI*) and canopy vegetation greenness ($NDVI_{up}$)? if the latter holds, we might be able to develop upscaling algorithms for $Thermal_{ground}$ and $NDVI_{down}$ in tropical landscapes.

2. Material and Methods

2.1 Study Area

Fieldwork was implemented in the KwaZulu-Natal province of South Africa between April 7th and April and April 22nd 2018 (Fig. 1). We concentrated our field campaigns on the coastal landscapes, which comprise fragments of coastal forests remaining after long-term historical and recent forest loss (Olivier, van Aarde & Lombard, 2013), large tree plantations, small patches of natural grasslands and croplands. The forests represent the southernmost end of East African Tropical Coastal Forest which extends from tropical central Africa along the east African coast (Burgess, Clarke & Rodgers, 1998). They occur within the Maputaland-Pondoland-Albany biodiversity hotspot and the Maputaland Centre of Plant Endemism (Wyk & Smith, 2001), which support high levels of floristic endemism as well as a number of narrowly endemic species, including relict species. The climate of the study region is humid and sub-tropical, with annual rainfall since 1976 averaging 1336 ± 117 mm $year^{-1}$.

2.2 Data collection and processing

We sampled 35 plots for habitat quality attributes, i.e. measuring $Thermal_{ground}$ using a Optris PI450 Thermal Imaging Camera (382 x 288 Pixels, 29 ° lens angle, 0.04 K thermal resolution, 7.5 - 13 µm spectral range) and $NDVI_{down}$ as normalised difference vegetation index (NDVI) using a MAPIR camera with filters for the Red (660 nm) and Near-Infrared (850 nm) parts of the electromagnetic spectrum (16 MP sensor: 4608 x 3456 Pixels, 82° HFOV (23mm) f/2.8 Aperture. We measured *LAI* and *FCover* using hemispherical photography using a Canon 5D Mark II with a Sigma f2.8 fisheye lens and $NDVI_{up}$ using the MAPIR camera facing upwards. The time of measurement during the day is likely to affect the results for $Thermal_{ground}$ measurements (Senior et al., 2018). We aimed to minimise the impact of time of day as confounding factor

by acquiring the majority of data at similar times, and primarily between 10 am and 2 pm (surrounding peak day time temperatures and solar gain). Weather did not change over considerably the field period (sunny with occasional clouds during data recordings) minimising weather impacts as confounding factor on modelled relationships. Whilst appropriate for the purpose of this study, our data can only be understood as temporal snapshots of ground surface temperature variations.

2.2.1 Sampling Design

Plots were set up in 6 main habitat types along transects stretching across habitat edges (Fig. 2). We sampled a total of 11 transects (Supporting Information, Table S1): six transects across natural forest – edge – natural grassland habitats (T01, T02, T07-T10), four transects stretching across natural forest – edge – *Eucalyptus* plantation habitats (T03-T06) and one transect stretching across natural forest –edge - natural grassland – bush habitats (T11). Forests comprised three different forest types: coastal lowland forest, scarp forest and peatland forest. Each transect comprised three plots (one per habitat type) except for T11, which comprised five plots.

We sampled an additional five forest plots and seven woodland plots to increase sampling effort for canopy structure measurements needed for the upscaling.

2.2.2 Collection of habitat quality data

We acquired fisheye images in habitat quality plots of 20 m x 20 m dimensions followed standard protocols (Pfeifer, 2015). In brief, at each plot, we took on average 12 high-resolution images through a digital camera and equipped with a hemispherical (fish-eye) lens with sampling points distributed within the plot (Fig. 2a) following the VALERI design (VAlidation of Land European Remote Sensing Instruments) and hence standard protocols developed for the Global LAI Project (Pfeifer, 2015). The camera was held at 1 m above ground, looking vertically upward from beneath the canopy. The levelled hemispherical photographs were acquired normal to a local horizontal datum, orienting the optical axis of the lens to local zenith.

155 NDVI images (*JPGs) were acquired using a MAPIR Survey 2 NDVI Red and NIR camera. We
156 acquired NDVI images of the ground vegetation greenness (pointing the NDVI camera downward,
157 $\boldsymbol{NDVI_{down}}$) and of canopy greenness (pointing the NDVI camera upwards, $\boldsymbol{NDVI_{up}}$). We also acquired an
158 image of the MAPIR ground target (i.e. targets of known reflectance values) at the start of each survey and
159 we repeated this throughout the day if sky conditions changed. We acquired $\boldsymbol{NDVI_{down}}$ and $\boldsymbol{NDVI_{up}}$ images
160 at five sample points for each plot. Ground images were acquired using a 50 x 50 cm square made of metal
161 rulers to delineate boundaries around each point (Fig. 2a). At each sampling point, we also measured
162 $Thermal_{ground}$ as radiometric corrected values (saved as snapshots in *csv matrix format) pointing the
163 thermal camera downwards, again using the 50 x 50 cm grids made from metal rulers to indicate boundaries
164 around each sampling point. $Thermal_{ground}$ data acquisition failed for the grassland plot at T02, which was
165 excluded in relevant analyses.
166
167 2.2.3 Processing of habitat quality data
168 Leaf area index (sensu Plant Area Index, *LAI*, corrected for foliage clumping) was estimated from the
169 fisheye images at plot level. Fractional vegetation cover (sensu canopy closure, *FCover*, in %) was
170 estimated for each image and hence sampling point. Fisheye images were first processed using in house
171 algorithms (available for download from the Global LAI Project websites:
172 https://globallai.wordpress.com/publications/) and the freeware CAN-EYE v 6.3.8 (Weiss & Baret, 2010),
173 following steps outlined in Pfeifer et al. 2012. In brief, the in-house algorithms extracted the blue band from
174 each fisheye image as the blue band achieves maximum contrast between leaf and sky. This is because
175 absorption of leafy materials is maximal and sky scattering tends to be highest in that band (Jonckheere,
176 Muys & Coppin, 2005a). The algorithm then applied the global Ridler & Calvard method (Ridler &
177 Calvard, 1978) to the blue band extracted from each image for identifying the optimal brightness threshold
178 that distinguishes vegetation from sky (Jonckheere, Muys & Coppin, 2005b). The algorithm then used the
179 threshold derived for each image to create binary images of vegetation and sky from the blue band images,
180 which were subsequently processed in the canopy analysis software CAN-EYE V6.3.8 (Weiss & Baret,

2010: http://www.paca.inra.fr/can_eye) limiting the field of view of the lens to values between 0 and 60° to avoid mixed pixels and thus misclassifications.

Each NDVI image was calibrated using the MAPIR Plugin (https://github.com/mapircamera/QGIS) within the spatial analysis software Quantum GIS v2.14.3. The plugin first loads the ground target image to find the calibration values. It then calibrates all survey images using those values. We subsequently processed calibrated NDVI images and thermal images to summary statistics using R statistical software following steps outlined in table 1. For some samples and plots, calibration produced non-sensible results for $NDVI_{down}$ and those samples and plots were excluded from the relevant analyses (the forest plots in T02 - T05 and T07 and the plantation plot in T03). The errors resulted from missing at-plot ground target images preventing us from calibrating images accurately.

2.3 Statistical analyses of habitat quality data

We used linear modelling to test for relationships between $NDVI_{down}$ and $NDVI_{up}$ and between $NDVI_{down}$ and *FCover* expecting that higher canopy greenness and closure would increasingly diminish light availability on the floor thereby hampering below-canopy vegetation growth and greenness. Specifically, we tested for mean, minimum and maximum of $NDVI_{down}$ as a function of mean, minimum and maximum of $NDVI_{up}$ as well as *FCover*. We also used linear modelling to test for relationships between *FCover* and $Thermal_{ground}$ and between *LAI* and $Thermal_{ground}$, expecting that mean and maximum ground surface temperatures are declining with increasing *FCover* and *LAI*, which act to filter out sun light and to prevent vertical mixing of air below the vegetation canopy (Hardwick et al., 2015). To visualise key relationships, we used *ggplot* in R statistical software package using the smoothing function specifying linear or general additive model dependencies.

We used pairwise Wilcoxon tests with Bonferroni adjustments to test for significant differences in summary statistics of $NDVI_{up}$, $NDVI_{down,}$ *FCover*, *LAI* and $Thermal_{ground}$ between habitat types sampled. We expected higher values of $NDVI_{down}$ and $Thermal_{ground}$ corresponding with lower values of *FCover* and *LAI* in open habitat types such as bushland and edges compared to forest interior and *Eucalyptus* plantations.

207

208 2.4 Upscaling habitat quality data using Landsat imagery

209 We focused on Landsat Surface Reflectance Satellite Level-2 satellite product, i.e. satellite images that are
210 freely available online, of high geospatial accuracy, and can be downloaded as surface reflectance data for
211 comparisons over time and space (and hence are already corrected for atmospheric noise).

212 We used two Landsat scenes acquired over the study landscape on June 4th in 2014. We used those
213 images to upscale canopy structure data, specifically canopy leaf area index and fractional vegetation cover
214 derived from the hemispherical images. To increase sample size for the developing of the upscaling models,
215 we used hemispherical images acquired in May 2015 and May 2018 from random locations across the
216 coastal landscape. We assumed that canopy structure did not change significantly for the plots sampled,
217 which is a reasonable assumption given the plots were located in woody ecosystems from little utilised
218 shrubs to coastal forests, the majority being located within protected areas.

219 We downloaded the Landsat 8 surface reflectance product (LASRC), derived from the Landsat 8
220 Operational Land Imagery data in each Landsat scene, from the USGS Earth Explorer after screening for
221 clouds aiming to minimise cloud coverage over the landscape. We processed those reflectance data by
222 setting pixels covered with clouds or haze to NA and only using pixels for which the pixel quality attributes
223 indicated clear conditions (i.e. pixel quality attributes coded as 322, 386, 834, 898, or 1346) and excluding
224 water bodies. We mosaicked the four scenes and cropped the extent of the raster mosaic to the study area.
225 Reflectance data were used to compute three maps of vegetation greenness (i.e. the normalised difference
226 vegetation index, NDVI (Tucker, 1979) , the modified soil-adjusted vegetation index, MSAVI2 (Qi et al.,
227 1994), and the two-band enhanced vegetation index, EVI2 (Jiang et al., 2008). We used the 'raster'
228 (Hijmans & van Etten, 2010) and 'glcm' (Zvoleff, 2014) packages in R statistical software to obtain texture
229 indices MEAN and DISSIMILARITY from a grey-level co-occurrence matrix each for the red, near-
230 infrared and shortwave infrared 1 bands. These computations were implemented on each matrix with a 90
231 degree shift, with 64 grey-levels for the matrix and a window size of 3 × 3 pixels following Pfeifer et al.

2016. We also computed mean and standard deviation maps of NDVI using the focal function in the *raster* package specifying a moving window size of 8 pixels (Hijmans & van Etten, 2010).

To map canopy structure, we combined canopy structure data acquired in 2015 with canopy structure data acquired during this fieldwork yielding a total of 115 plots measured for canopy *LAI* and *FCover* (with N = 96 forest plots, 14 woodland plots, 16 bush plots, 10 forest edge plots, 24 plantation plots (including broad-leaved and needle leaved plantation) and 7 crop plots. We extracted reflectance, texture and vegetation greenness data onto each plot. We developed random forest models linking spectral, texture and vegetation greenness data to canopy structure data after excluded predictor variables from the model that were highly inter-correlated ($P > 0.6$). We computed the models using the *randomForest* package in R (Table 2: final predictor variables included in predictive model).

We subsequently used the final models to upscale plot measured canopy attributes to landscape scale excluding water bodies and any other NA regions from the resulting maps. To exclude water bodies, we computed a non-habitat map from the two Landsat scenes. We processed reflectance data by setting pixels representing water bodies (i.e. pixel quality attributes coded as 324, 388, 836, 900, or 1348).

3. Results

3.1 Habitat quality variation between habitat types

Habitats differed significantly in habitat quality metrics measured in this study (Fig. 3). As expected, $Thermal_{ground}$ decreased significantly from grassland and bush plots to edge plots ($P < 0.05$) and then to forest plots ($P < 0.001$). $Thermal_{ground}$ for sampling points in plantation plots was significantly higher than for sampling points in forest plots and significantly lower than for sampling points in grassland and bush plots ($P < 0.01$). $NDVI_{down}$ showed different trends with habitat types compared to $Thermal_{ground}$ and was significantly higher in grassland, bush and plantation plots compared to edge and forest plots ($P < 0.05$). *FCover* was significantly higher for edge, forest and woodland plots compared to plantation plots and significantly lower in woodland versus forest plots (pairwise Wilcoxon tests with Bonferroni adjustment (*P*

257 < 0.05). However, variance within habitats was significantly different (Levene test for variance
258 homogeneity significant at $P < 0.001$). $NDVI_{up}$ was significantly lower in plantation plots compared to
259 forest plots ($P < 0.05$) and was marginally higher in bush compared to edge plots ($P = 0.052$). Canopy *LAI*
260 did not differ significantly between habitats.
261
262 3.2 Habitat quality attributes and their inter-relationships
263 $Thermal_{ground}$ and $NDVI_{down}$ showed significant linear dependencies on canopy closure (Table 3, Figures 4
264 and 5). Specifically, for each increase in *FCover* by 10%, $Thermal_{ground}$ declined by 0.6°C starting from
265 27.2°C (Fig. 4) and for each increase in *LAI* by 1 unit, $Thermal_{ground}$ declined by 1°C decrease starting from
266 26.6°C (Fig. 5). For each increase in in *FCover* by 10%, $NDVI_{down}$ declined by 0.1 starting from 0.80 (Fig.
267 4) and for each increase in *LAI* by 1 unit, $NDVI_{down}$ declined by 0.14 starting from 0.80 (Fig. 5). For the
268 latter, however, the pattern only held when measured between habitat types and disappeared when looking
269 at forest plots only.
270 Contrary to expectations $NDVI_{down}$ increased significantly with increasing $NDVI_{up}$ with an approximate
271 0.08 increase in ground NDVI for each 0.1 increase in canopy NDVI. $Thermal_{ground}$ showed no relationship
272 with canopy NDVI. Finally, $Thermal_{ground}$ and $NDVI_{down}$ are not independent of each other and data suggest
273 that for each increase in canopy NDVI by 0.1, ground surface temperature increased by approximate 0.4°C.
274 This pattern held despite an expected influence of measurements acquired during different times of the day
275 (i.e. measurement bias through sampling effect). Plots those $Thermal_{ground}$ was higher than expected from
276 their $NDVI_{down}$ include in particular grassland plots measured during peak temperatures of the day (a, c, d).
277 Plots those $Thermal_{ground}$ was lower than expected from their $NDVI_{down}$ include a grassland plot from Ngoye
278 (b) and a forest plot from Enseleni (e), both measured early in the day (cooler time of the day).
279
280 3.3 Mapping habitat quality using upscaling algorithms
281 The predictive capacity of the habitat quality mapping using Landsat reflectance data and derived indices
282 was limited. Random forest models explained 34 % of the variability on the *LAI* data and 33% in the

variability of *FCover* data (Table 2). We used the resulting *LAI* maps and *FCover* maps to map ground surface temperature and ground NDVI (Fig. 6) using models as detailed in the legends for Figures 4 for and 5.

4. Discussion

Ground surface temperature and ground NDVI, both habitat attributes that have been linked to diversity, abundance and behaviour of animal species in different studies, are positively correlated. Both statistically and significantly link to canopy structure attributes commonly mapped using remote sensing data. Specifically, opening canopies by about 20% or reducing canopy leaf area by 1, would result in an increase of average temperatures on the ground by more than 1°C and an increase in ground vegetation greenness by 0.2 and 0.14 respectively.

These findings are not surprising based on the mechanistic understanding of radiation fluxes within vegetation layers (Deardorff, 1978; Best, 1998). They are likely to have important implications for microclimate within forests stands though, as tropical forests are changing rapidly with current global change drivers. Forest canopies are increasingly showing stress and die-back responses to repeated droughts, the latter often acting in concert with other disturbance drivers to open forest canopies in positive feedbacks to increase tree mortality (Malhi et al., 2009). Disturbance has been shown to decrease canopy in the Amazon rainforests by 13% to 60% depending on disturbance intensity (*FCover* = 98% in intact forests, 85 % in logged and lightly burned forests, 63% in heavily logged forests and 39% in heavily logged and burned forests) (Gerwing, 2002). Similarly, rainforests in Malaysian Borneo show decreased canopy cover even ten years after logging and conversion to palm stands with *FCover* being 6 to 10% lower in logged forests compared to primary forests and 25% in established oil palm stands compared to primary forests (Pfeifer et al., 2016). Based on statistical relationships derived in this study, these canopy cover declines would translate to increases in ground surface temperature of at least 3°C in severely disturbed forests. Our results are in line with findings from a recent review on the buffering impact of forests, in which warming effects caused by land use change ranged from +1.1°C in degraded forests to +2.7°C in

plantations, +6.2°C in pasture and +7.6°C in cropland (Senior et al., 2018). Taking into account expectations on temperature extremes during the day (Blonder et al. 2018) may paint an even bleaker picture as stronger responses of temperature extremes to canopy structure changes would be expected (Ewers and Banks-Leite, 2013; Hardwick et al., 2015).

Pronounced changes in ground surface temperatures following canopy changes are likely to contribute - directly or indirectly - to changes in species diversity and distribution (Varner & Dearing, 2014; Kaspari et al., 2015) and in species' ecological roles within forest ecosystem processes (Ewers et al., 2015). These effects are likely to be stronger for species in the tropics and in particular tropical ectotherms (Deutsch et al., 2008; Potter, Arthur Woods & Pincebourde, 2013; Kaspari et al., 2015). Tropical insects are suggested to track air temperatures close to their optimal temperature but also to have narrow thermal tolerances; they experience near-lethal temperatures faster than temperate insects and warming is expected to reduce their population fitness by up to 20% (Deutsch et al., 2008). Ground surface temperature adds to the heat stress effect as the operational temperature of ectotherms is determined by both convection (the exchange of energy between body and air) and conductance (the direct transfer of energy between objects and surfaces) (Potter, Arthur Woods & Pincebourde, 2013). However, direct empirical evidence is rare and we suggest a couple of steps following on from this pilot study.

First, ground surface temperature should be sampled together with air temperature throughout the course of the day and over several days, and if necessary seasons (e.g. dry versus wet seasons in the Afrotropics), which could be achieved using mini meteorological dataloggers and radiation sensors This will allows to capture variation in average temperature and temperature extremes as experienced by species in the forest understorey. Second, the tropical forest floor harbours a set of insect taxa believed to be distinct from the forest canopy (Stork & Grimbacher, 2006b). Their abundance and distribution on the ground is probably linked to leaf litter (Rodgers & Kitching, 1998), ground vegetation , availability of host plants (Hill et al., 1995; Novotny et al., 2002) as well as microclimate (Schulze, Linsenmair & Fiedler, 2001). Thus, detailed species community and species behavioural studies looking at a gradient of surface temperatures along a gradient of canopy openness should be implemented for a range of taxonomic groups.

Third, habitat quality can have different meanings to species depending on the ecological scales they operate on and their interlinkages in trophic networks (Schulze, Linsenmair & Fiedler, 2001). For example, ground-dwelling insects feeding on detritus may be more affected by fine scale variation in temperature (Levesque, Fortin & Mauffette, 2002; Lessard, Dunn & Sanders, 2009). In contrast, larger body-sized mobile bird species acquiring resources across larger spatial scales may be more affected by the availability of nesting places and the distribution of prey items in the landscape (Sekercioglu et al., 2007). Network analyses are rare, in particular for the tropics, but would allow us to determine whether changes in insects and ground vegetation due to microclimate changes are likely to propagate into changes in larger-body sized animal groups.

5. Conclusions

Accounting for micro-scale variation in temperature is seen as essential to improve biodiversity impact predictions using species distribution models (Suggitt et al., 2011). Thermal imaging of land surfaces can be implemented using unmanned aerial vehicles (Bellvert et al., 2014) and to some extent satellite sensors (Lee et al., 2015). However there are technical challenges in flying UAVs across many regions and changes in temperature below vegetation canopies ('buffer effect') would be difficult to detect. Our ground-based analyses show that canopy structure and below canopy ground surface temperatures show clear significant relationships, which could be exploited for mapping habitat quality metrics that matter to species. However, more work is needed to (1) reduce uncertainties in these relationships and (2) to improve canopy structure mapping (and hence subsequent ground surface temperature mapping) using remote sensing data. Our data seem to suggest that increasing sampling effort to capture spatial (along gradients of canopy cover and leaf area) and temporal (as function of day light, climate seasonality and climate extremes) variation in ground surface temperature would be beneficial to address the first point. The second point could be addressed by using data acquired at higher spatial resolution, as we have shown for forest degradation gradients in Borneo (Pfeifer et al., 2016) and by sampling canopy structure variation for a wide range of habitat types on the ground resolution. Either way, linking ground surface temperature (maps) to species demographic traits and

abundance distributions in predictive biodiversity modelling (Pfeifer et al., 2017) would be the next essential step to truly determine the choice of ground surface temperatures as suitable habitat quality metric. This could then be exploited to design landscapes that maximise benefits from habitat restoration and management for biodiversity conservation and other ecosystem services.

Acknowledgements

The Royal Society enabled the implementation of this pilot study supported under project grant number *Research Grants 2017 Round 1 - RG160847*. We acknowledge the logistic support of M.A.P. Scientific Services (https://www.mapss.co.za/, Pretoria, info@mapss.co.za) in the field.

References

Von Arx G., Dobbertin M., Rebetez M. 2012. Spatio-temporal effects of forest canopy on understory microclimate in a long-term experiment in Switzerland. *Agricultural and Forest Meteorology*. DOI: 10.1016/j.agrformet.2012.07.018.

Bale JS., Masters GJ., Hodkinson ID. et al. 2002. Herbivory in global climate change research: direct effects of rising temperature on insect herbivores. *Global Change Biology* 8:1–16. DOI: 10.1046/j.1365-2486.2002.00451.x.

Barçante L., M. Vale M., Maria MA. 2017. Altitudinal migration by birds: a review of the literature and a comprehensive list of species. *Journal of Field Ornithology* 88:321–335. DOI: 10.1111/jofo.12234.

Bellvert J., Zarco-Tejada PJ., Girona J., Fereres E. 2014. Mapping crop water stress index in a 'Pinot-noir' vineyard: comparing ground measurements with thermal remote sensing imagery from an unmanned aerial vehicle. *Precision Agriculture* 15:361–376. DOI: 10.1007/s11119-013-9334-5.

Best MJ. 1998. A Model to Predict Surface Temperatures. *Boundary-Layer Meteorology* 88:279–306. DOI: 10.1023/A:1001151927113.

Blonder, B., Both, S., Coomes, D. et al. In Press. Extreme and highly heterogeneous microclimates in selectively logged tropical forests. *Frontiers in Forests and Global Change*.

387 Bromham L., Cardillo M., Bennett AF., Elgar MA. 1999. Effects of stock grazing on the ground
388 invertebrate fauna of woodland remnants. *Austral Ecology* 24:199–207. DOI: 10.1046/j.1442-
389 9993.1999.00963.x.
390 Burgess ND., Clarke GP., Rodgers WA. 1998. Coastal forests of eastern Africa: Status, endemism
391 patterns and their potential causes. *Biological Journal of the Linnean Society 64,* 337-367. DOI:
392 10.1006/bijl.1998.0224.
393 Chaplin-Kramer R., Sharp RP., Mandle L. et al. 2015. Spatial patterns of agricultural expansion
394 determine impacts on biodiversity and carbon storage. *Proceedings of the National Academy of*
395 *Sciences of the United States of America* 112:7402–7. DOI: 10.1073/pnas.1406485112.
396 Deardorff JW. 1978. Efficient prediction of ground surface temperature and moisture, with inclusion of a
397 layer of vegetation. *Journal of Geophysical Research* 83:1889. DOI: 10.1029/JC083iC04p01889.
398 Deutsch CA., Tewksbury JJ., Huey RB. et al. 2008. Impacts of climate warming on terrestrial ectotherms
399 across latitude. *Proceedings of the National Academy of Sciences of the United States of America*
400 105:6668–72. DOI: 10.1073/pnas.0709472105.
401 Didham RK., Lawton JH. 1999. Edge Structure Determines the Magnitude of Changes in Microclimate
402 and Vegetation Structure in Tropical Forest Fragments1. *Biotropica* 31:17–30. DOI:
403 10.1111/j.1744-7429.1999.tb00113.x.
404 Ewers RM., Banks-Leite C. 2013. Fragmentation Impairs the Microclimate Buffering Effect of Tropical
405 Forests. PLoS ONE 8, e58093. doi:10.1371/journal.pone.0058093.
406 Ewers RMRM., Boyle M., Gleave RARA. et al. 2015. Logging cuts the functional importance of
407 invertebrates in tropical rainforest. *Nature communications* 6:6836. DOI: 10.1038/ncomms7836.
408 Gerwing JJ. 2002. Degradation of forests through logging and fire in the eastern Brazilian Amazon.
409 *Forest Ecology and Management* 157:131–141. DOI: 10.1016/S0378-1127(00)00644-7.
410 Gibson L., Lee TM., Koh LP., et al. 2011. Primary forests are irreplaceable for sustaining tropical
411 biodiversity. *Nature* 478:378–81. DOI: 10.1038/nature10425.
412 Gilliam FS. 2007. The Ecological Significance of the Herbaceous Layer in Temperate Forest Ecosystems.

BioScience 57:845–858. DOI: 10.1641/B571007.

Godfray HCJ., Beddington JR., Crute IR. et al. 2010. Food Security: The Challenge of Feeding 9 Billion People. *Science* 327:812–818. DOI: 10.1126/science.1185383.

Hadi., Pfeifer M., Korhonen L., Wheeler C., Rautiainen M. 2017. Forest canopy structure and reflectance in humid tropical Borneo: A physically-based interpretation using spectral invariants. *Remote Sensing of Environment* 201. DOI: 10.1016/j.rse.2017.09.018.

Hardwick SR., Toumi R., Pfeifer M., Turner EC., Nilus R., Ewers RM. 2015. The relationship between leaf area index and microclimate in tropical forest and oil palm plantation: Forest disturbance drives changes in microclimate. *Agricultural and Forest Meteorology* 201. DOI: 10.1016/j.agrformet.2014.11.010.

Hemmings Z., Andrew NR. 2017. Effects of microclimate and species identity on body temperature and thermal tolerance of ants (Hymenoptera: Formicidae). *Austral Entomology* 56:104–114. DOI: 10.1111/aen.12215.

Hijmans RJ., van Etten J. 2010. raster: Geographic analysis and modeling with raster data. *R package version* 1:r948.

Hill JK., Hamer KC., Lace LA., Banham WMT. 1995. Effects of Selective Logging on Tropical Forest Butterflies on Buru, Indonesia. *The Journal of Applied Ecology* 32:754. DOI: 10.2307/2404815.

Jiang Z., Huete AR., Didan K., Miura T. 2008. Development of a two-band enhanced vegetation index without a blue band. *Remote Sensing of Environment* 112:3833–3845. DOI: 10.1016/j.rse.2008.06.006.

Jonckheere IG., Muys B., Coppin PR. 2005a. Derivative analysis for in situ high dynamic range hemispherical photography and its application in forest stands. *Geoscience and Remote Sensing Letters, IEEE* 2:296–300.

Jonckheere I., Muys B., Coppin P. 2005b. Allometry and evaluation of in situ optical LAI determination in Scots pine: a case study in Belgium. *Tree Physiology* 25:723–732.

Kaspari M., Clay NA., Lucas J., Yanoviak SP., Kay A. 2015. Thermal adaptation generates a diversity of

thermal limits in a rainforest ant community. *Global Change Biology* 21:1092–1102. DOI: 10.1111/gcb.12750.

Lee CM., Cable ML., Hook SJ., Green RO., Ustin SL., Mandl DJ., Middleton EM. 2015. An introduction to the NASA Hyperspectral InfraRed Imager (HyspIRI) mission and preparatory activities. *Remote Sensing of Environment* 167:6–19. DOI: 10.1016/J.RSE.2015.06.012.

Lessard J-P., Dunn RR., Sanders NJ. 2009. Temperature-mediated coexistence in temperate forest ant communities. *Insectes Sociaux* 56:149–156. DOI: 10.1007/s00040-009-0006-4.

Levesque KR., Fortin M., Mauffette Y. 2002. Temperature and food quality effects on growth, consumption and post-ingestive utilization ef.ciencies of the forest tent caterpillar Malacosoma disstria (Lepidoptera: Lasiocampidae). *Bulletin of Entomological Research* 92:127–136. DOI: 10.1079/BER2002153.

Malhi Y., Aragão LE., Galbraith D. et al. 2009. Exploring the likelihood and mechanism of a climate-change-induced dieback of the Amazon rainforest. *Proceedings of the National Academy of Sciences* 106:20610–20615.

Matthews S. 2005. The water vapour conductance of Eucalyptus litter layers. *Agricultural and Forest Meteorology* 135, 73–81. doi:10.1016/j.agrformet.2005.10.004

Mcguire LP., Boyle WA. 2013. Altitudinal migration in bats: Evidence, patterns, and drivers. *Biological Reviews* 88:767–786. DOI: 10.1111/brv.12024.

Meijide A., Badu CS., Moyano F., Tiralla N., Gunawan D., Knohl A. 2018. Impact of forest conversion to oil palm and rubber plantations on microclimate and the role of the 2015 ENSO event. *Agricultural and Forest Meteorology* 252:208–219. DOI: 10.1016/J.AGRFORMET.2018.01.013.

Mortelliti A., Amori G., Boitani L. 2010. The role of habitat quality in fragmented landscapes: a conceptual overview and prospectus for future research. *Oecologia* 163:535–547. DOI: 10.1007/s00442-010-1623-3.

Novotny V., Basset Y., Miller SE., Weiblen GD., Bremer B., Cizek L., Drozd P. 2002. Low host specificity of herbivorous insects in a tropical forest. *Nature* 416:841–844. DOI: 10.1038/416841a.

465 Olivier PI., van Aarde RJ., Lombard AT. 2013. The use of habitat suitability models and species-area
466 relationships to predict extinction debts in coastal forests, South Africa. *Diversity and Distributions*
467 19:1353–1365. DOI: 10.1111/ddi.12099.
468 Pettorelli N., Wegmann M., Skidmore A. et al. 2016. Framing the concept of satellite remote sensing
469 essential biodiversity variables: challenges and future directions. *Remote Sensing in Ecology and*
470 *Conservation* 2, 122-131. doi:10.1002/rse2.15
471 Pfeifer M. 2015. *Manual to measure and model leaf area index and its spatial varaibility on local and*
472 *landscape scale*. Figshare. Fileset https://doi.org/10.6084/m9.figshare.5684182.v1
473 Pfeifer M., Gonsamo A., Disney M., Pellikka P., Marchant R. 2012. Leaf area index for biomes of the
474 Eastern Arc Mountains: Landsat and SPOT observations along precipitation and altitude gradients.
475 *Remote Sensing of Environment* 118, 103-115. doi:10.1016/j.rse.2011.11.009
476 Pfeifer M., Kor L., Nilus R., Turner E., Cusack J., Lysenko I., Khoo M., Chey VK., Chung AC., Ewers
477 RM. 2016. Satellites map the structure of Borneo's tropical forests across a degradation gradient.
478 *Remote Sensing of Environment* 176:84–97. DOI: 10.1016/j.rse.2016.01.014.
479 Pfeifer M., Lefebvre V., Peres CAA. et al. 2017. Creation of forest edges has a global impact on forest
480 vertebrates. *Nature* 551:187–191. DOI: 10.1038/nature24457.
481 Potter KA., Arthur Woods H., Pincebourde S. 2013. Microclimatic challenges in global change biology.
482 *Global Change Biology* 19:2932–2939. DOI: 10.1111/gcb.12257.
483 Qi J., Chehbouni A., Huete AR., Kerr YH., Sorooshian S. 1994. A modified soil adjusted vegetation
484 index. *Remote Sensing of Environment* 48:119–126. DOI: 10.1016/0034-4257(94)90134-1.
485 Rae DA., Armbruster WS., Edwards ME., Svengård-Barre M. 2006. Influence of microclimate
486 and species interactions on the composition of plant and invertebrate communities in alpine northern
487 Norway. *Acta Oecologica* 29:266–282. DOI: 10.1016/J.ACTAO.2005.11.007.
488 Retana J., Cerdá X. 2000. Patterns of diversity and composition of Mediterranean ground ant
489 communities tracking spatial and temporal variability in the thermal environment. *Oecologia*
490 123:436–444. DOI: 10.1007/s004420051031.

Ridler T., Calvard S. 1978. Picture thresholding using an iterative selection method. *IEEE transactions on Systems, Man and Cybernetics* 8:630–632.

Rodgers DJ., Kitching RL. 1998. Vertical stratification of rainforest collembolan (Collembola: Insecta) assemblages: description of ecological patterns and hypotheses concerning their generation. *Ecography* 21:392–400. DOI: 10.1111/j.1600-0587.1998.tb00404.x.

Royo AA., Collins R., Adams MB., Kirschbaum C., Carson WP. 2010. Pervasive interactions between ungulate browsers and disturbance regimes promote temperate forest herbaceous diversity. *Ecology* 91:93–105. DOI: 10.1890/08-1680.1.

Schulze CH., Linsenmair KE., Fiedler K. 2001. Understorey versus canopy: Patterns of vertical stratification and diversity among Lepidoptera in a Bornean rain forest. In: *Plant Ecology*. Springer, Dordrecht, 133–152. DOI: 10.1023/A:1017589711553.

Sekercioglu, C.H., Loarie, S.R., Oviedo Brenes, F., Ehrlich, P.R., Daily, G.C. 2007. Persistence of Forest Birds in the Costa Rican Agricultural Countryside. *Conservation Biology* 21:482–494. DOI: 10.1111/j.1523-1739.2007.00655.x.

Senior RA., Hill JK., Benedick S., Edwards DP. 2018. Tropical forests are thermally buffered despite intensive selective logging. *Global Change Biology*. DOI: 10.1111/gcb.13914.

Shirima DD., Pfeifer M., Platts PJ., Totland ?., Moe SR. 2015. Interactions between canopy structure and herbaceous biomass along environmental gradients in moist forest and dry miombo woodland of Tanzania. *PLoS ONE* 10. DOI: 10.1371/journal.pone.0142784.

Stork NE., Grimbacher PS. 2006. Beetle assemblages from an Australian tropical rainforest show that the canopy and the ground strata contribute equally to biodiversity. *Proceedings. Biological sciences* 273:1969–75. DOI: 10.1098/rspb.2006.3521.

Suggitt AJ., Gillingham PK., Hill JK. et al. 2011. Habitat microclimates drive fine-scale variation in extreme temperatures. *Oikos* 120:1–8. DOI: 10.1111/j.1600-0706.2010.18270.x.

Tucker CJ. 1979. Red and photographic infrared linear combinations for monitoring vegetation. *Remote Sensing of Environment* 8:127–150. DOI: 10.1016/0034-4257(79)90013-0.

517 Varner J., Dearing MD. 2014. The importance of biologically relevant microclimates in habitat suitability
518 assessments. *PloS one* 9:e104648. DOI: 10.1371/journal.pone.0104648.
519 Wyk AE van., Smith GF. 2001. Regions of floristic endemism in Southern Africa: a review with
520 emphasis on succulents. ISBN 1919766189. Umdaus Press, Hatfield, South Africa.
521 Zvoleff A. 2014. Calculate textures from grey-level co-occurrence matrices(GLCMs) in R.
522
523

Figure 1(on next page)

Location of fieldwork in Kwa Zulu-Natal province, South Africa

In 2018, we sampled 35 plots for habitat quality attributes. Plots were set up in 6 main habitat types along transects stretching across habitat edges. We sampled a total of 11 transects. We sampled an additional five forest plots and seven woodland plots to increase sampling effort for canopy structure measurements needed for the upscaling. We used canopy structure data from additional forest and plantation plots sampled in 2015 (totalling 115 plots overall) to develop canopy structure maps (see Fig. 6). Photo credit: Marion Pfeifer.

Example of **habitat quality transects** in Ngoye Forest, South Africa

Natural grassland

Forest/Grassland Edge

0 100 200 300 400 m

Zoom on RapidEye

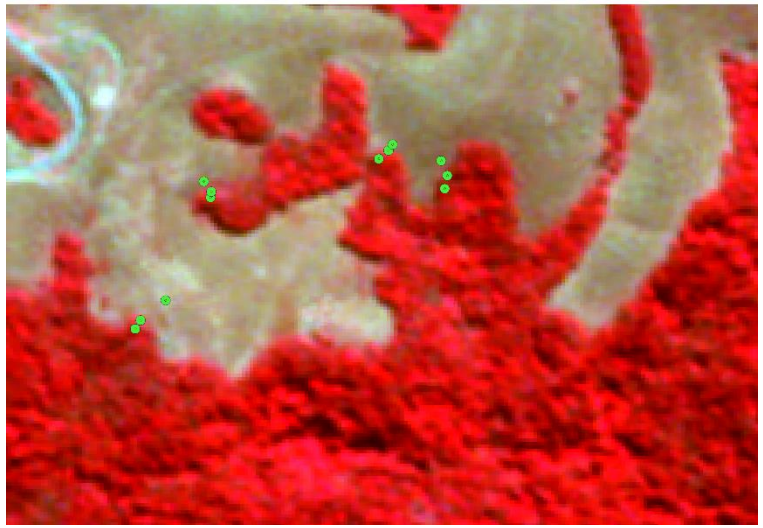

Forest

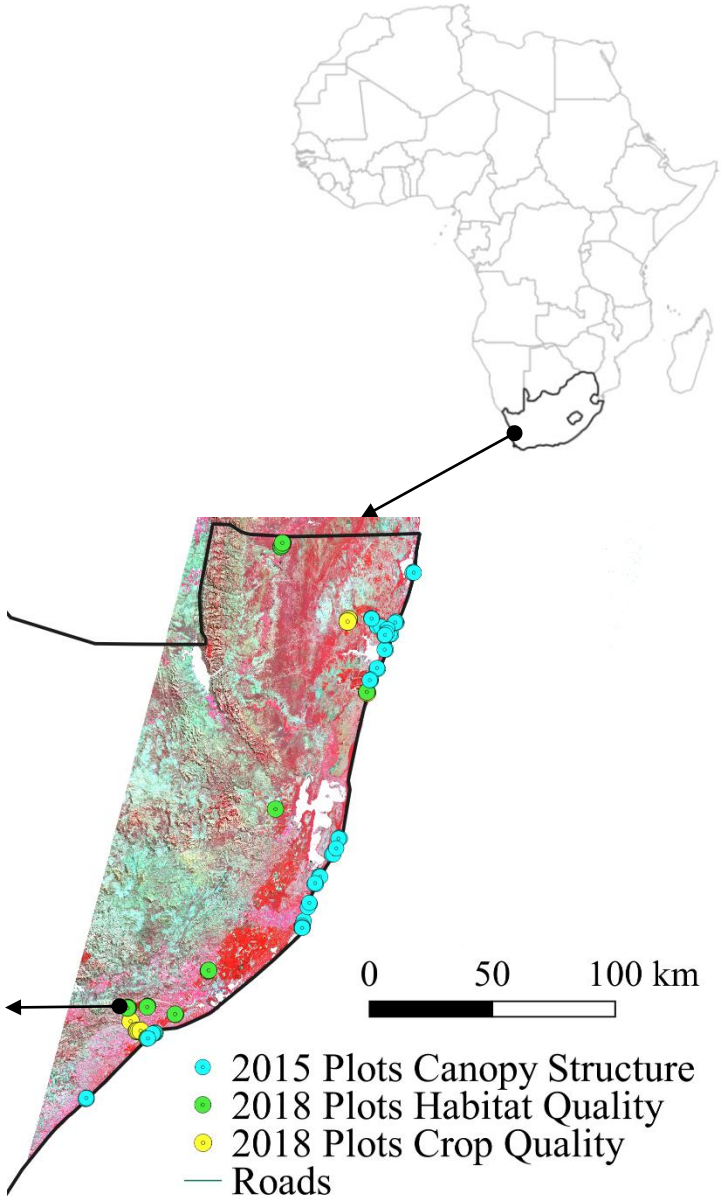

PeerJ Preprints | https://doi.org/10.7287/peerj.preprints.27168v1 | CC BY 4.0 Open Access | rec: 4 Sep 2018, publ: 4 Sep 2018

Figure 2(on next page)

Sampling design used during fieldwork.

(a) Plot sampling. We acquired $NDVI_{up}$, $NDVI_{down}$ and thermal images at five points per plot. We acquired fisheye images at 12 points per plot. (b) Location of plots along linear transects stretching across the edge between natural forests and matrix habitats. Darker shades indicate core areas of respective habitats.

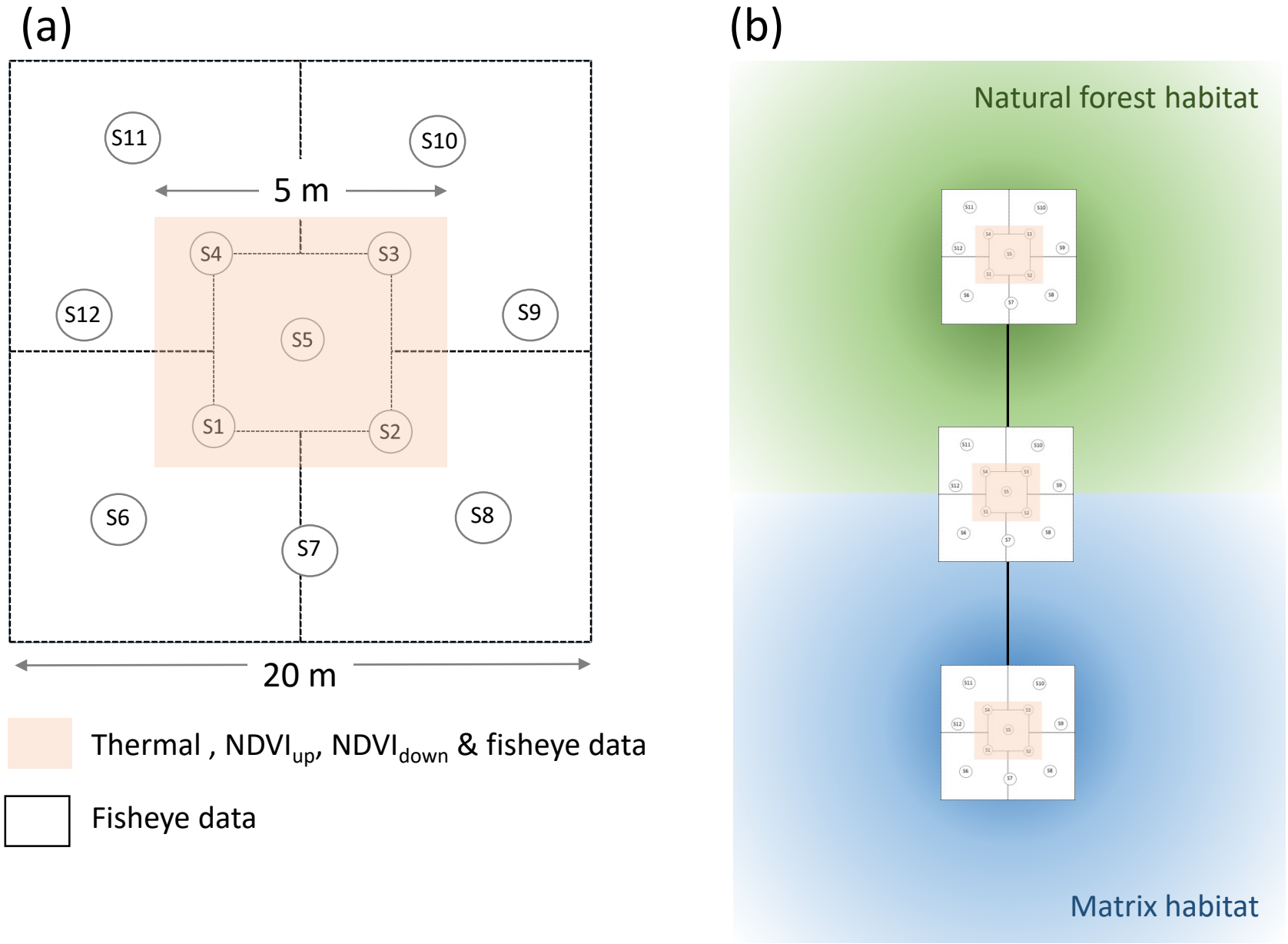

PeerJ Preprints | https://doi.org/10.7287/peerj.preprints.27168v1 | CC BY 4.0 Open Access | rec: 4 Sep 2018, publ: 4 Sep 2018

Figure 3(on next page)

Habitat quality attributes and their variation within and across habitat types.

Sample size differed between habitats. ***$NDVI_{down}$***: 144 points sampled across 29 plots (Grassland: 35 points from 7 plots, Bush: 5 points in 1 plots Edge: 54 points in 11 plots, Forest: 35 points in 7 plots and Plantation: 15 points from 3 plots). ***$Thermal_{ground}$***: 169 points sampled across 34 plots (Grassland: 30 points from 6 plots, Bush: 5 points in 1 plot, Edge: 54 points in 11 plots, Forest: 60 points in 12 plots and Plantation: 20 points from 4 plots). ***$NDVI_{up}$***: 139 points sampled across 28 plots (Bush: 5 points in 1 plots, Edge: 54 points in 11 plots, Forest: 60 points in 12 plots and Plantation: 20 points from 4 plots). ***FCover***: 528 points sampled across 40 plots (Bush: 15 points in 1 plots, Edge: 155 points in 11 plots, Woodland: 68 points in 7 plots, Forest: 230 points in 17 plots and Plantation: 60 points from 4 plots). ***LAI***: data are only estimated at plot level and hence shown for 1 bush plot, 11 edge plots, 7 woodland plots, 17 forest plots, and 4 plantation plots.

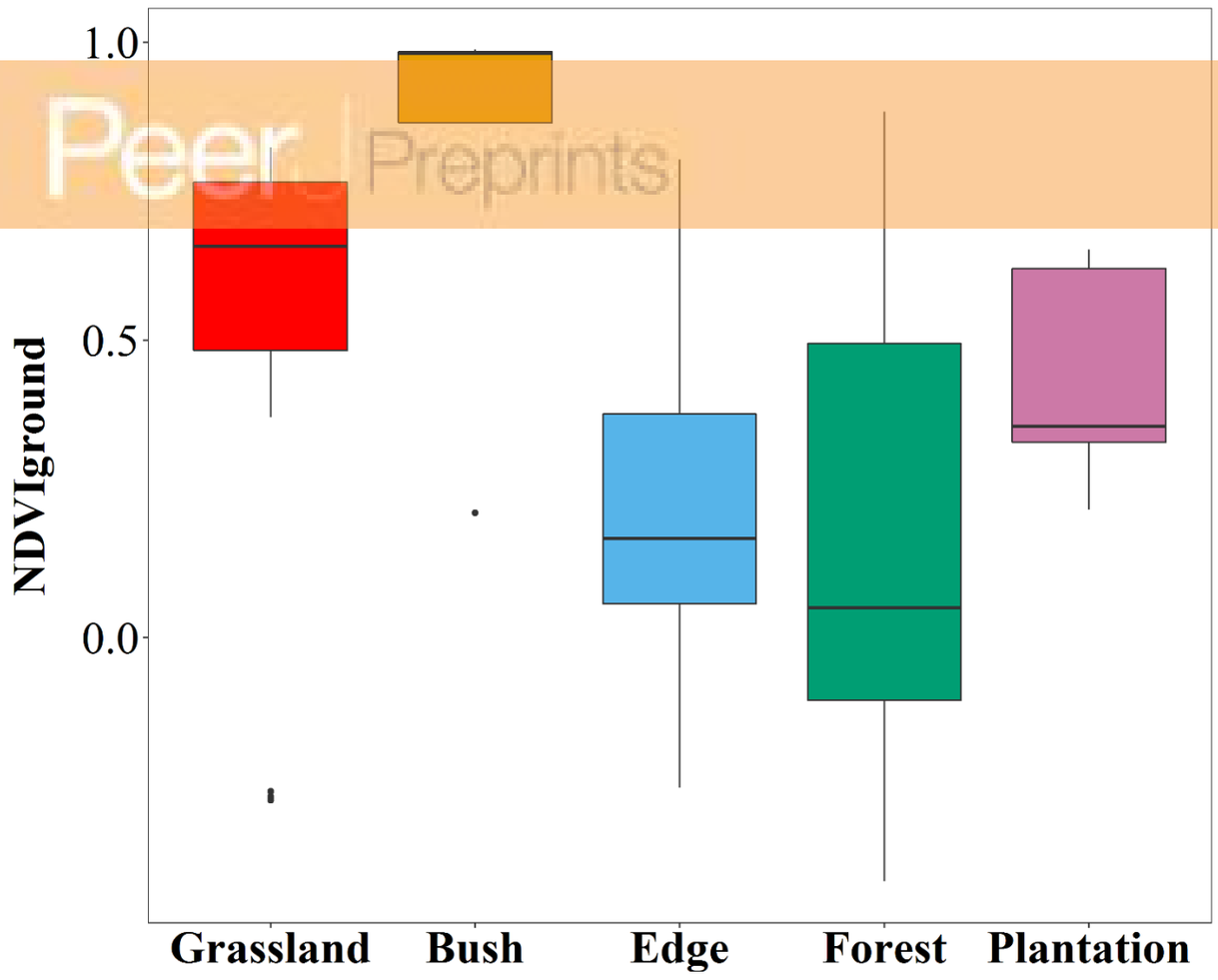

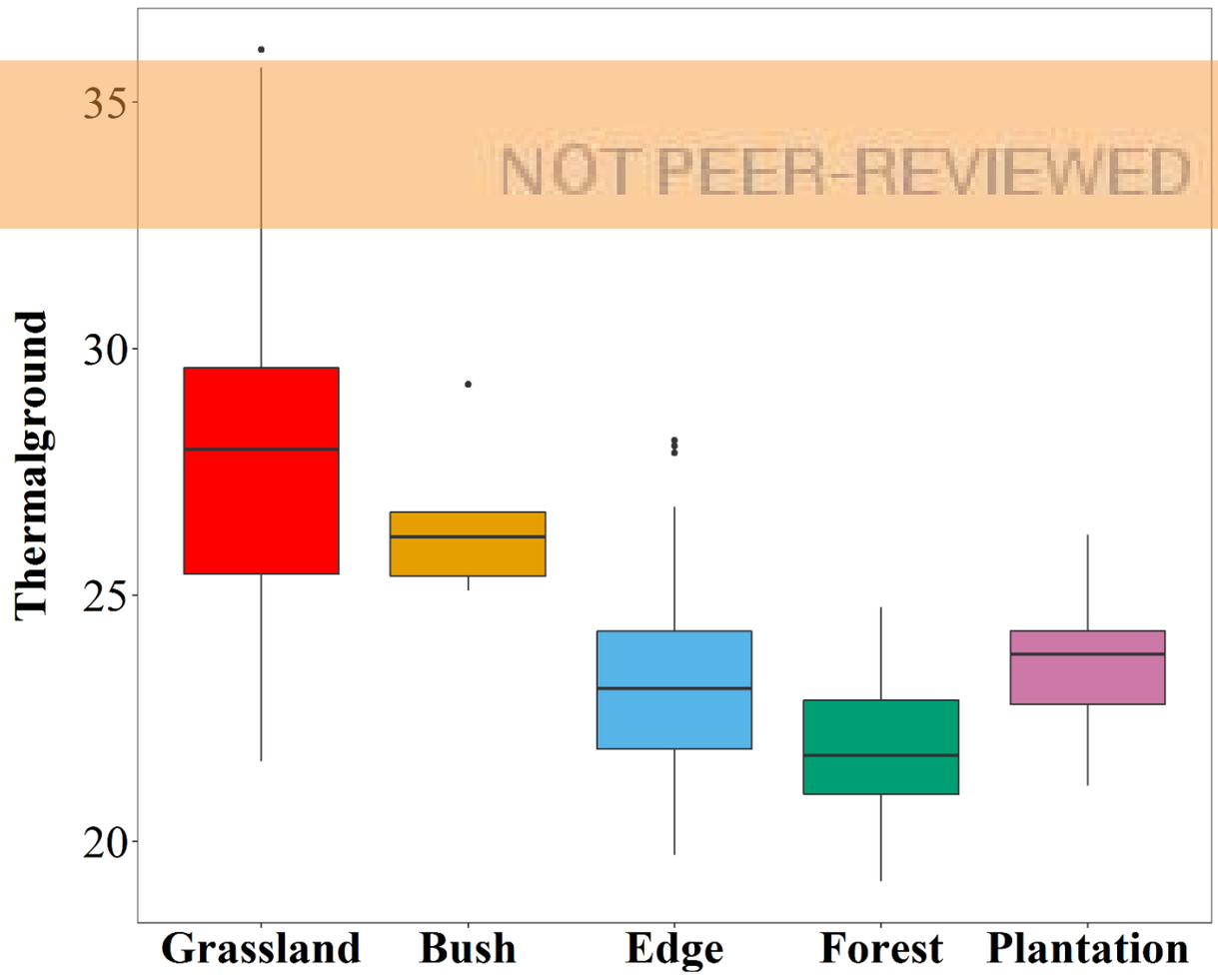

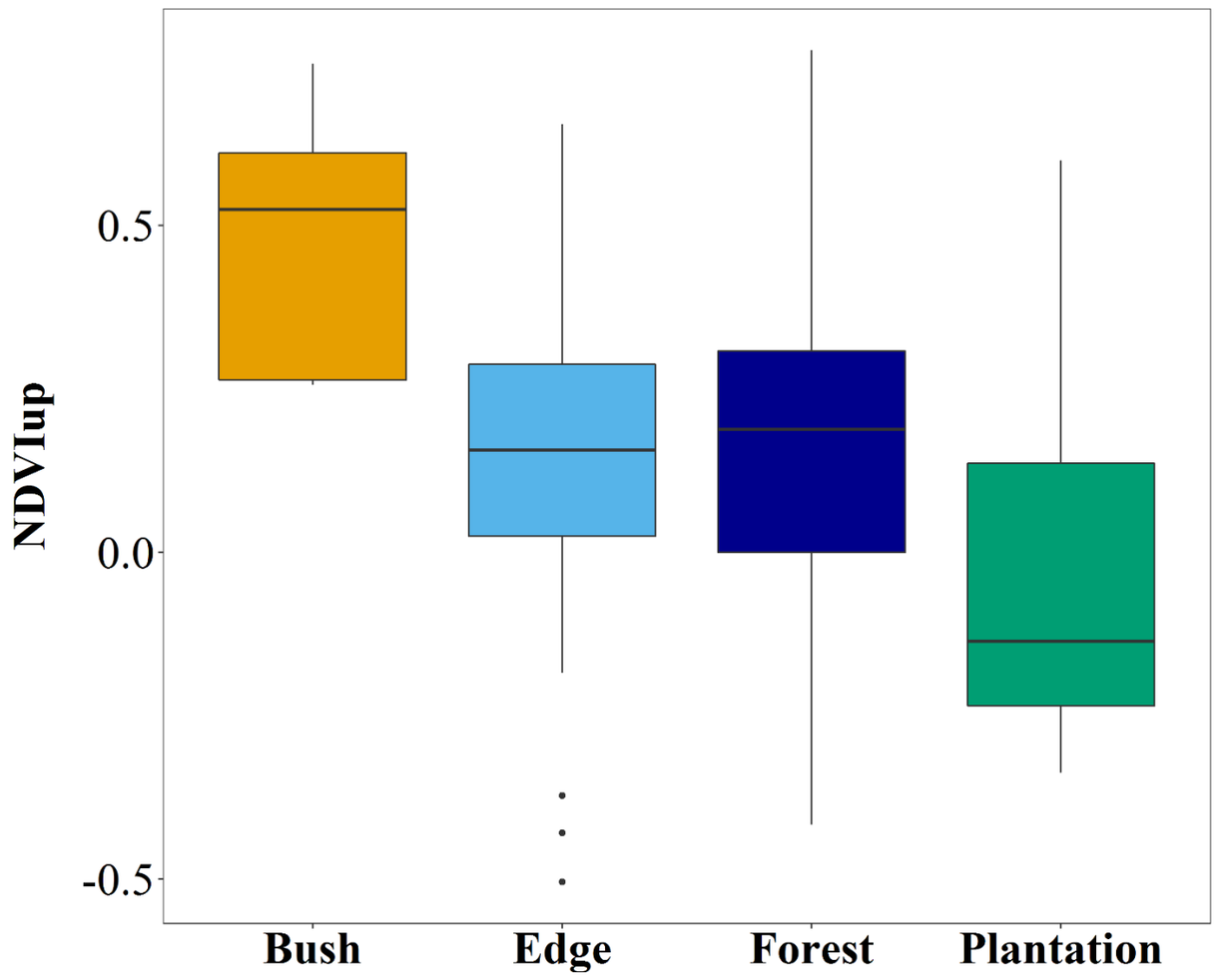

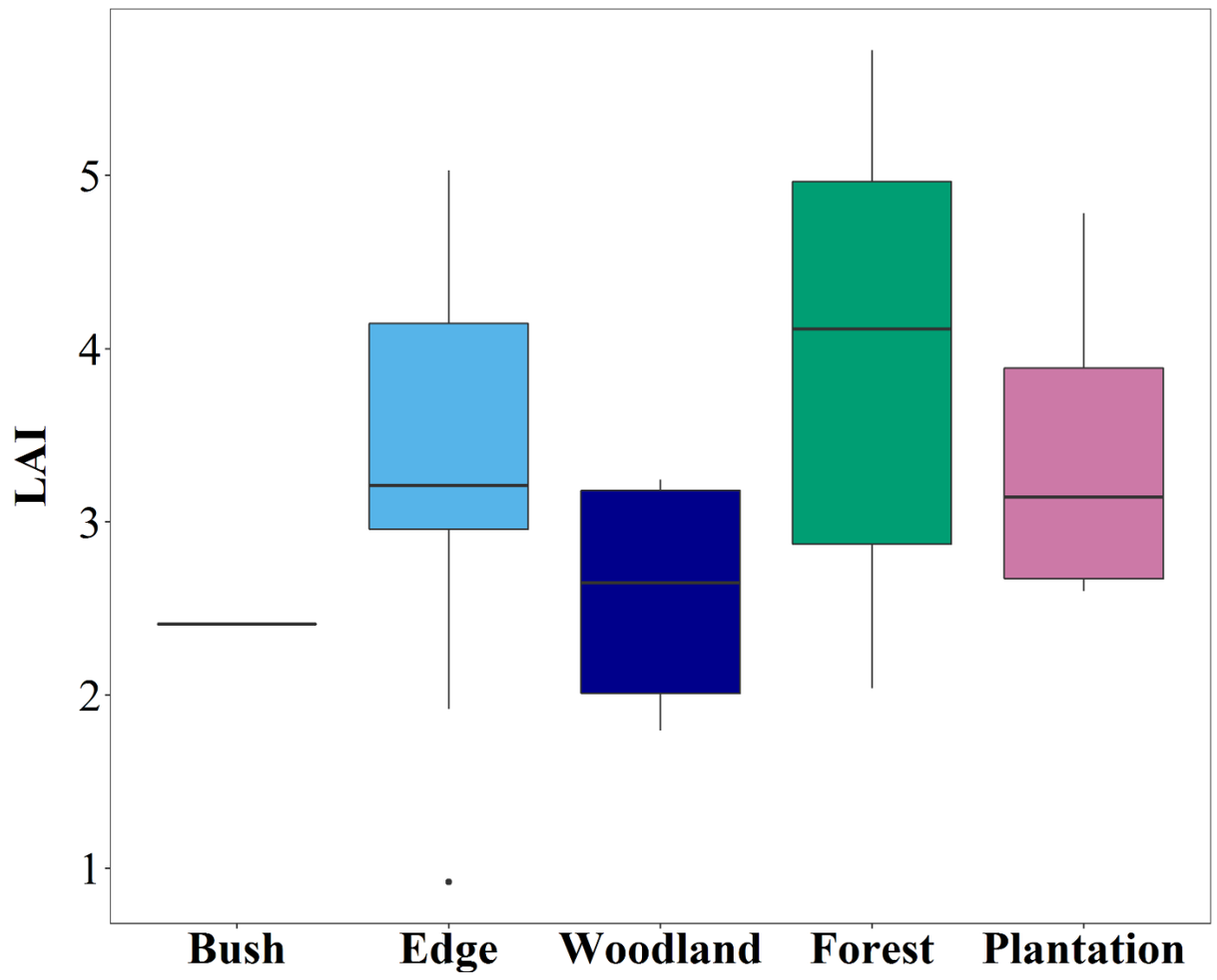

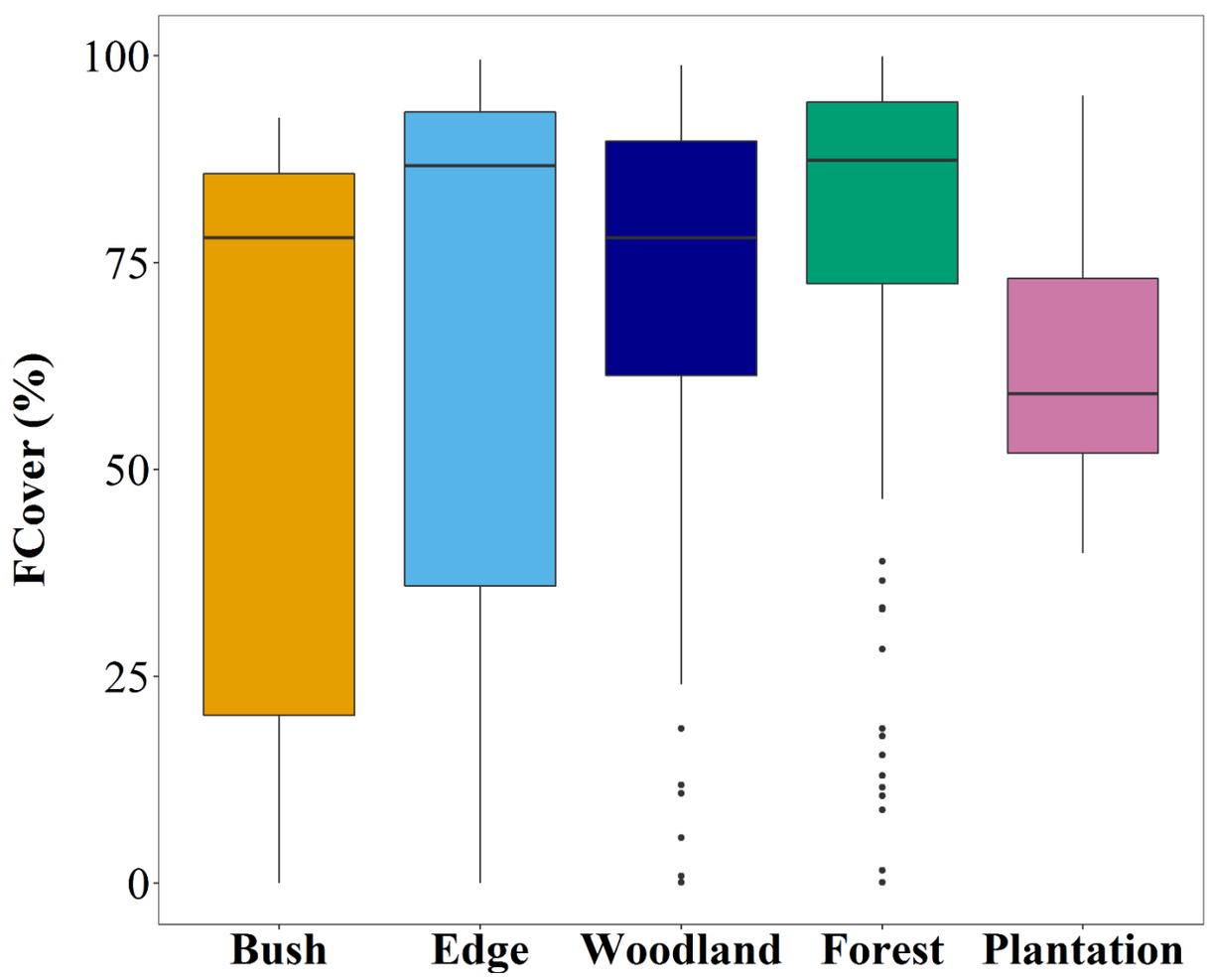

PeerJ Preprints | https://doi.org/10.7287/peerj.preprints.27168v1 | CC BY 4.0 Open Access | rec: 4 Sep 2018, publ: 4 Sep 2018

Figure 4(on next page)

Habitat quality attributes and their inter-relationships.

Model details shown with *** indicating P < 0.001, ** indicating *P* < 0.01 and * indicating *P* < 0.05. **Upper left**: $NDVI_{down}$ declined significantly with increasing *FCover* (N = 22, linear model: intercept = 0.98**, coefficient = -0.01**, R^2_{adj} = 0.33**). **Upper right**: $Thermal_{ground}$ also declined significantly with increasing canopy closure (N = 28, linear model: intercept = 27.20***, coefficient = -0.06**, R^2_{adj} = 0.30**). General additive models fitted the data slightly better with R^2_{adj} improving to 0.31***). **Lower left**: $NDVI_{down}$ increased significantly with increasing canopy greenness $NDVI_{up}$ (N = 22, linear model: intercept = 0.15*, coefficient = 0.75**, R^2_{adj} = 0.36**). General additive models better explained the relationship between $NDVI_{down}$ and $NDVI_{up}$ (R^2_{adj} = 0.51**). **Lower right**: $Thermal_{ground}$ increased significantly with increasing $NDVI_{down}$ (N = 28, linear model: intercept = 23.02***, coefficient = 3.97**, R^2_{adj} = 0.21**). Strong outliers from this relationship include (a) plot at Ngoye measured at midday during a hot and sunny day, (b) plot at Ngoye measured early in the morning, (c) plot at Enseleni Nature Reserve: patches of high grass and bare soil, and (d) degraded grassland plot with heavy grazing pressure at Sodwana Bay.

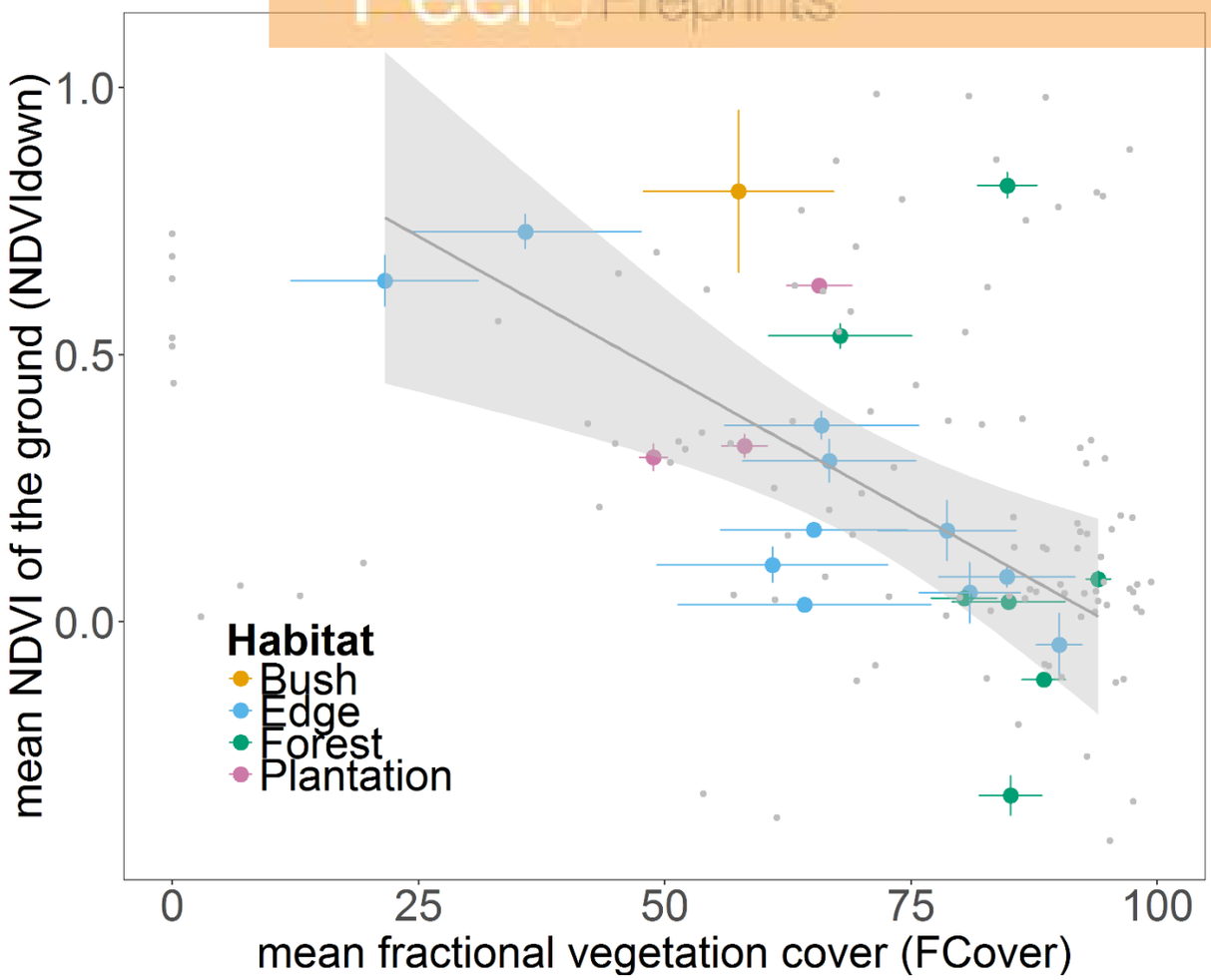

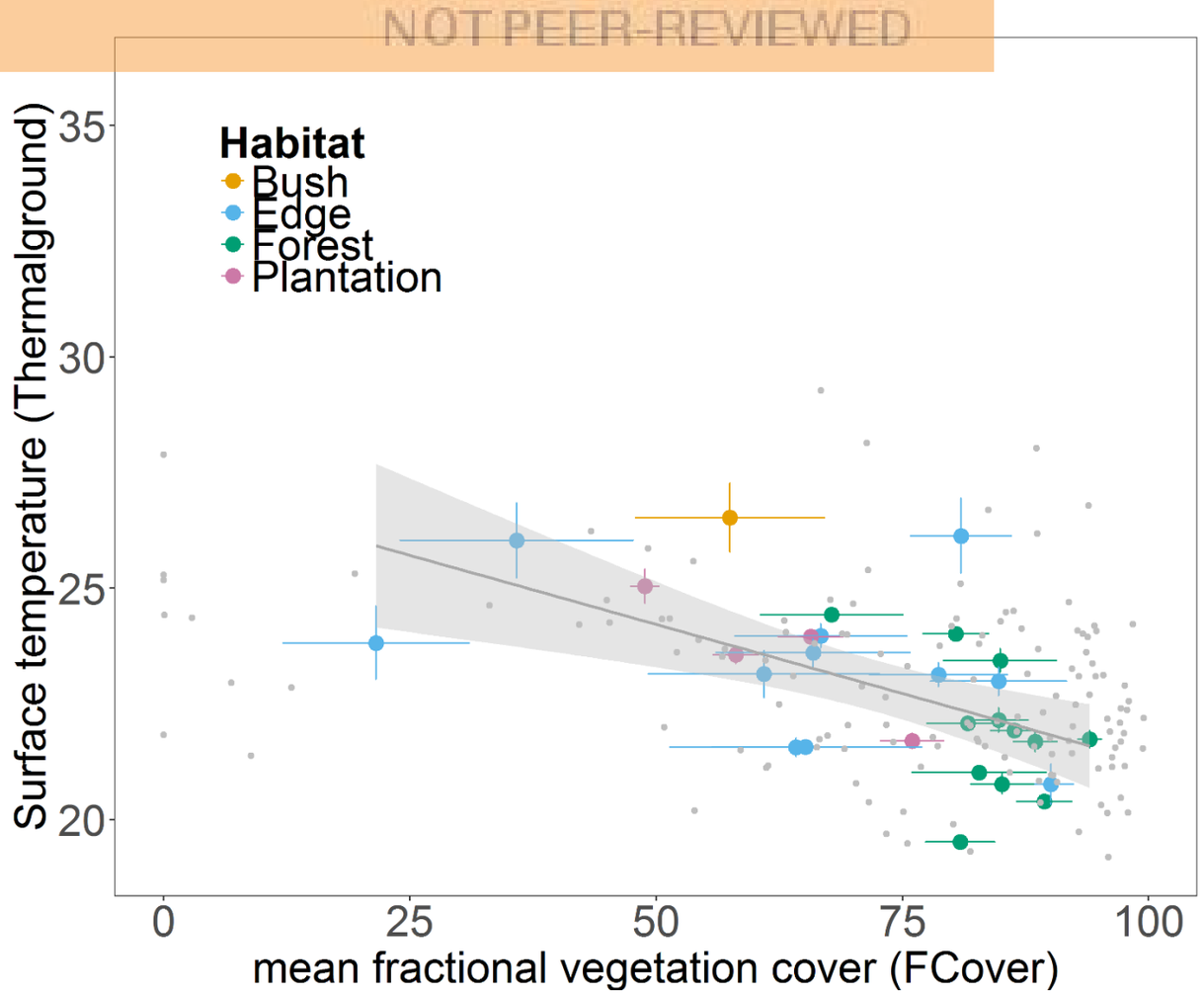

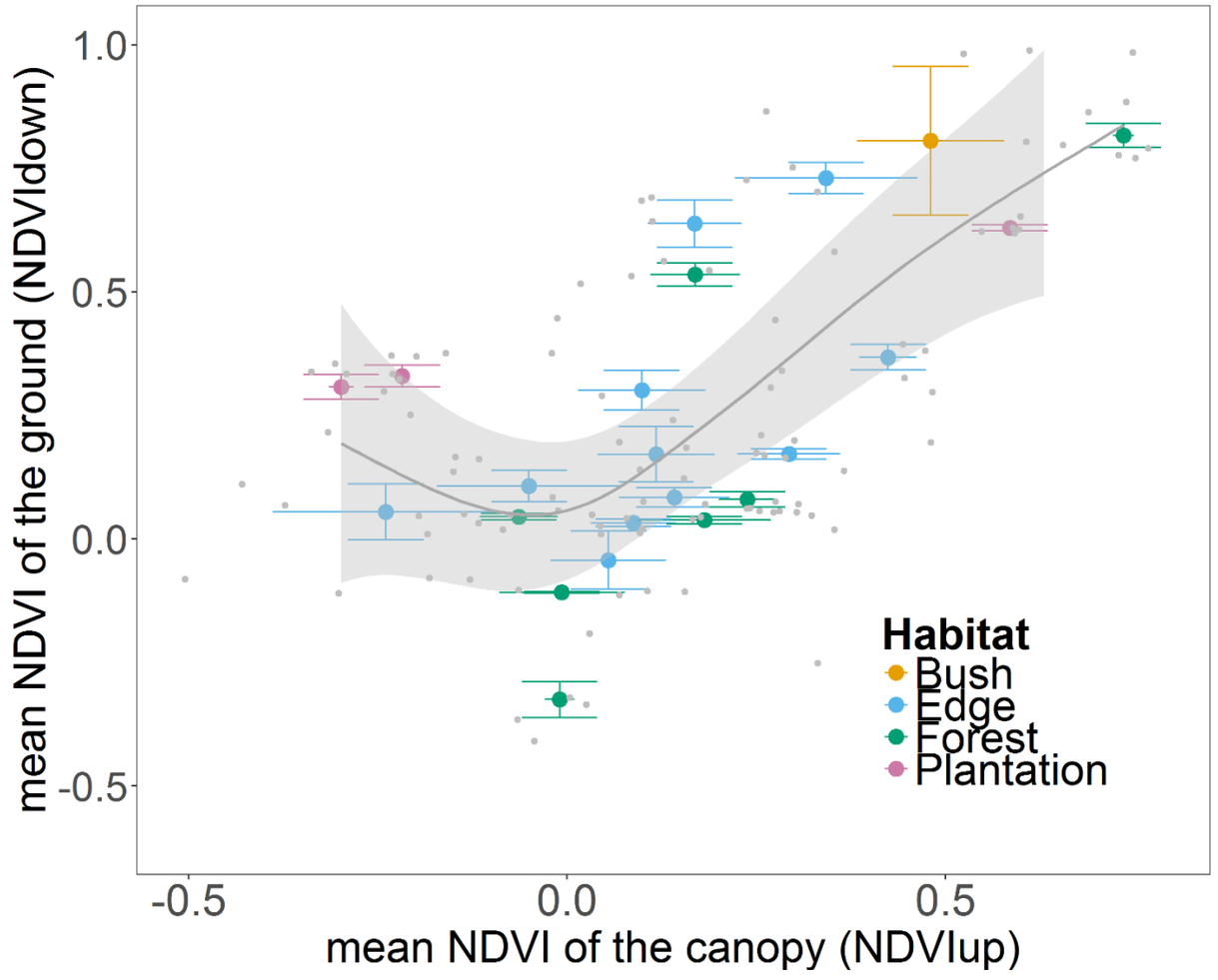

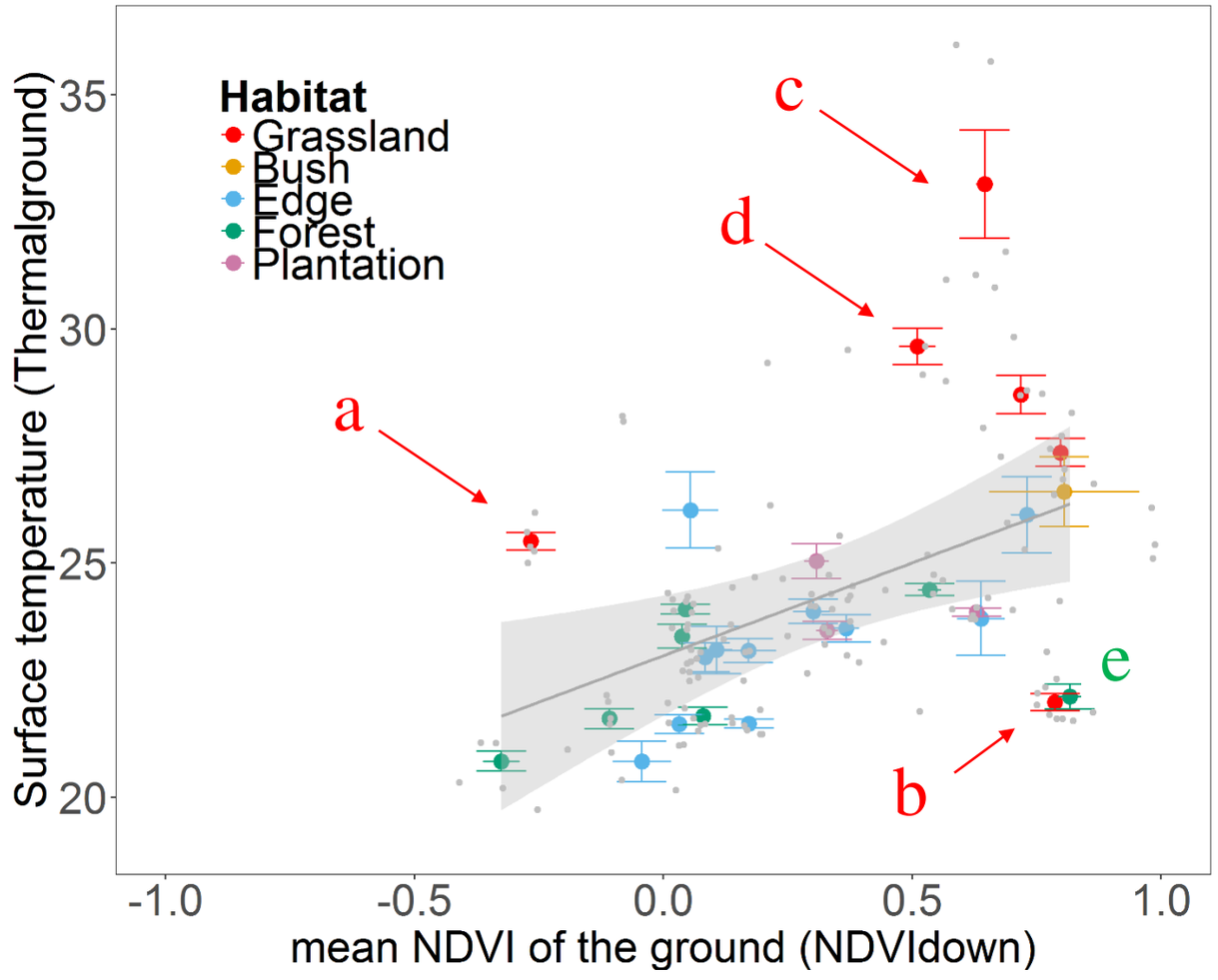

Figure 5(on next page)

Canopy LAI dependencies of ground surface temperature and ground NDVI.

Left: $NDVI_{down}$ declined significantly with increasing canopy leaf area (N = 22, linear model: intercept = 0.76**, coefficient = -0.14*, R^2_{adj} = 0.18*). **Right**: $Thermal_{ground}$ declined significantly with increasing canopy leaf area (N = 28, linear model: intercept = 26.63***, coefficient = -1.00***, R^2_{adj} = 0.35***).

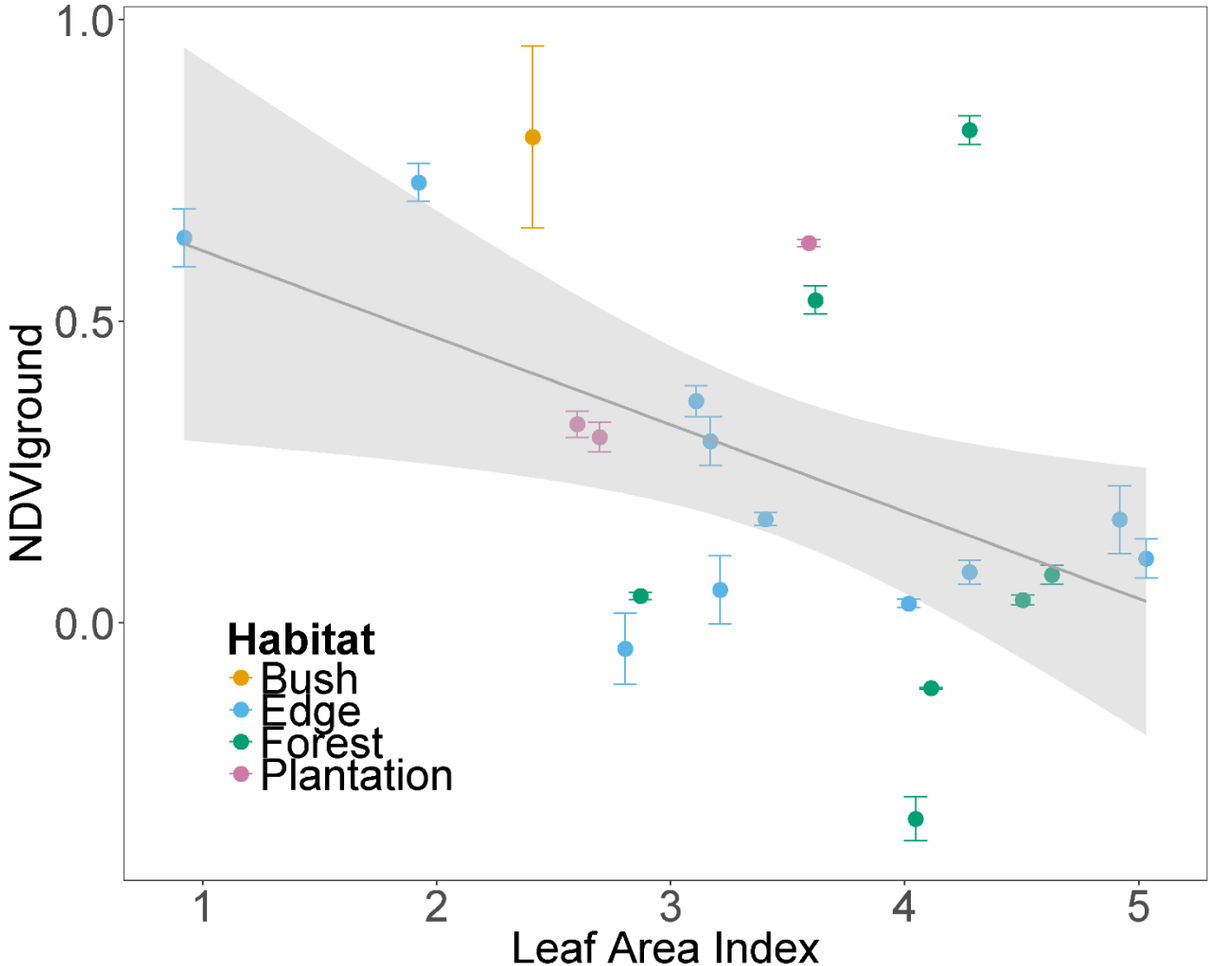

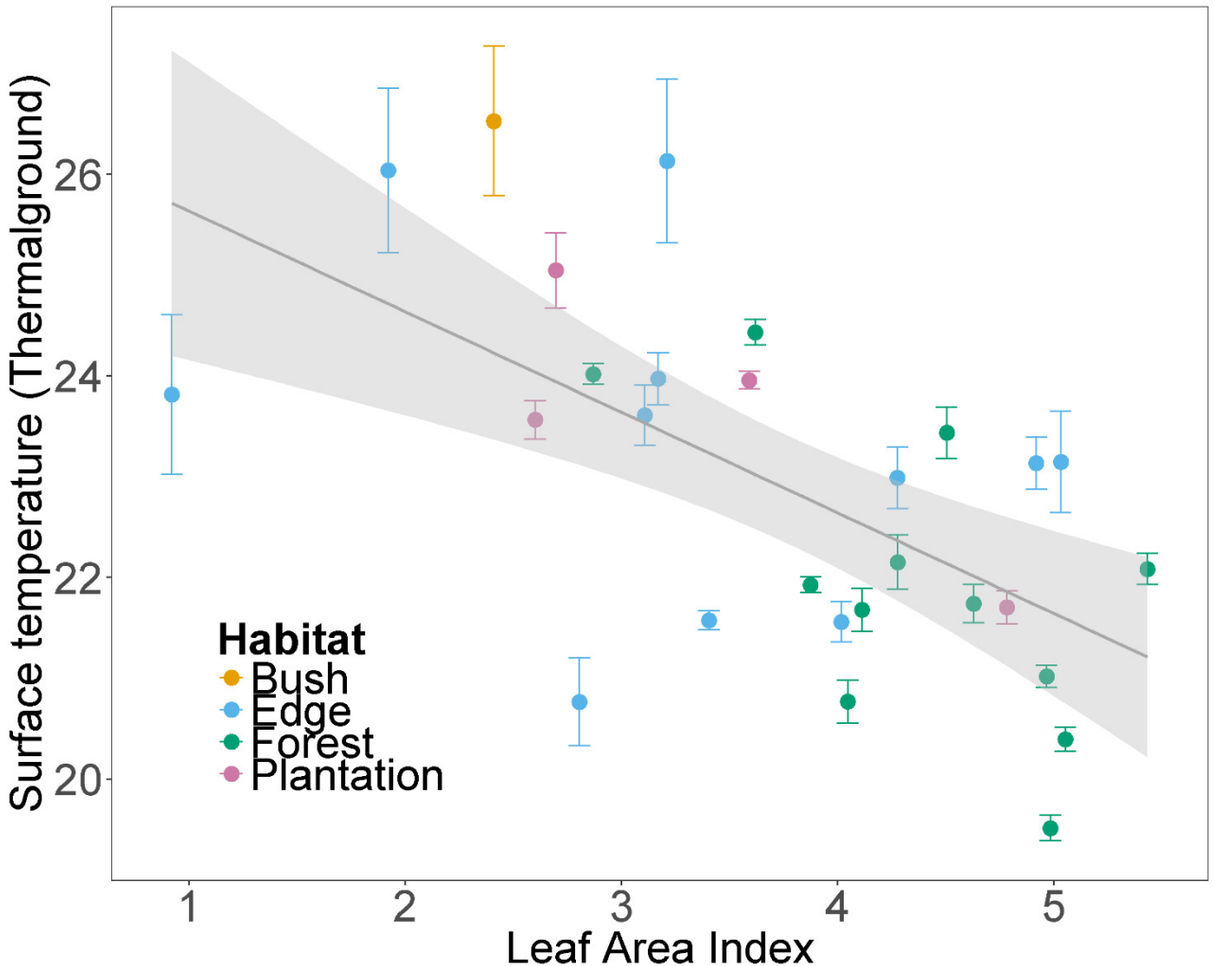

PeerJ Preprints | https://doi.org/10.7287/peerj.preprints.27168v1 | CC BY 4.0 Open Access | rec: 4 Sep 2018, publ: 4 Sep 2018

Figure 6(on next page)

Zoom into the *LAI* and derived $Thermal_{ground}$ maps as indicators of habitat quality.

The *LAI* map was developed using Landsat 8 sensor data with canopy *LAI* measurements acquired in plots in 2015 and 2018 using random forest models. The ground surface temperature map was derived from the *LAI* map using linear modelling (for details see Fig. 5). The zoom shows the Ngoye forest patch and surrounding human-modified landscapes that are predominantly growing sugarcane. The landscape stretches toward the coast featuring mosaics of tree plantations and natural forests. Photo credit: Marion Pfeifer.

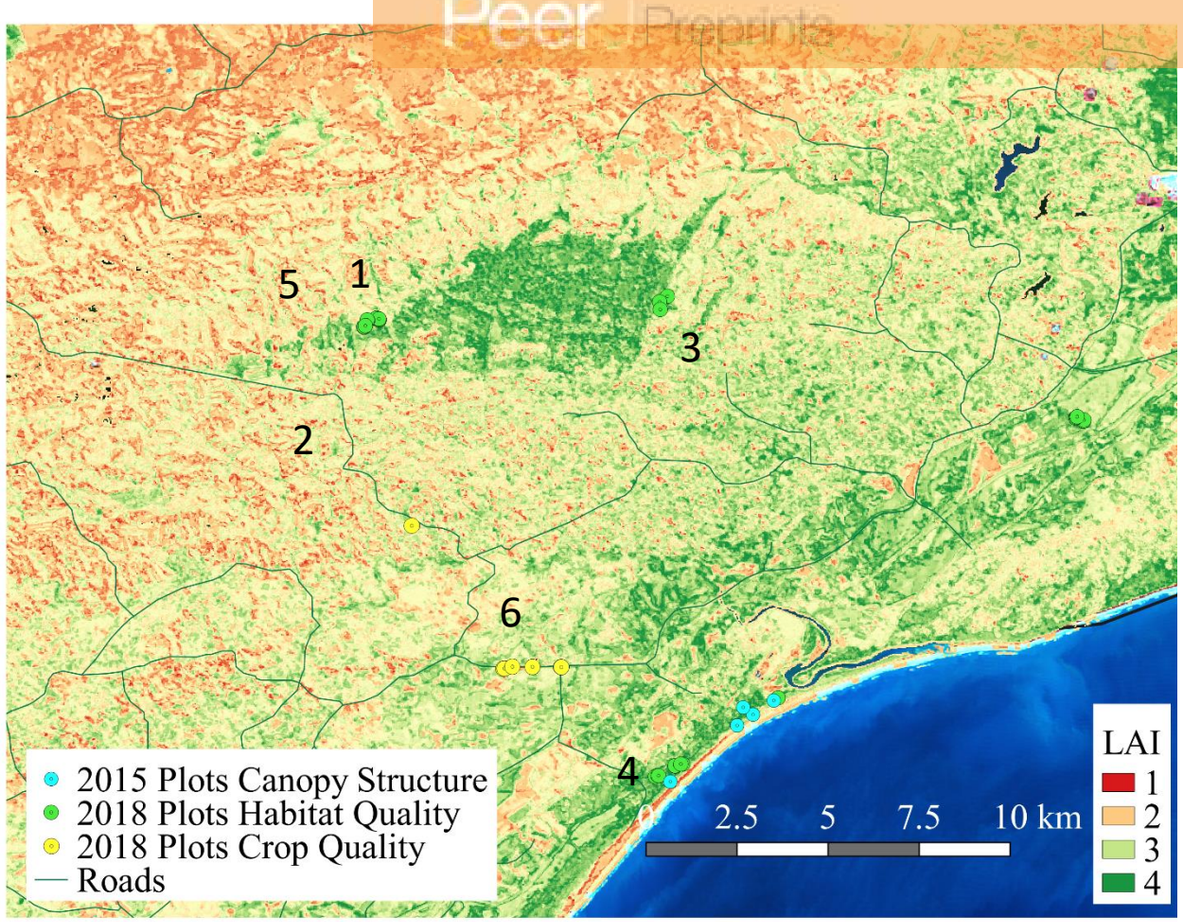

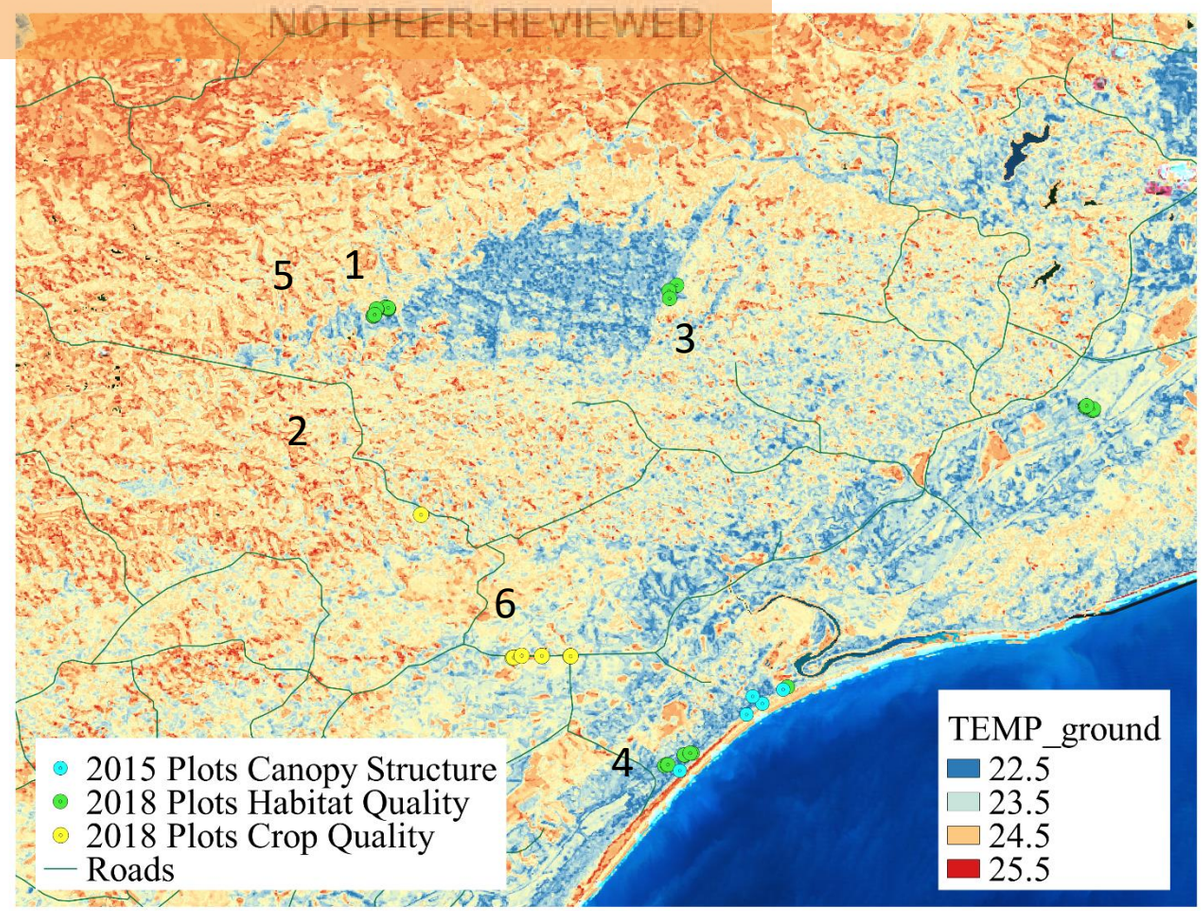

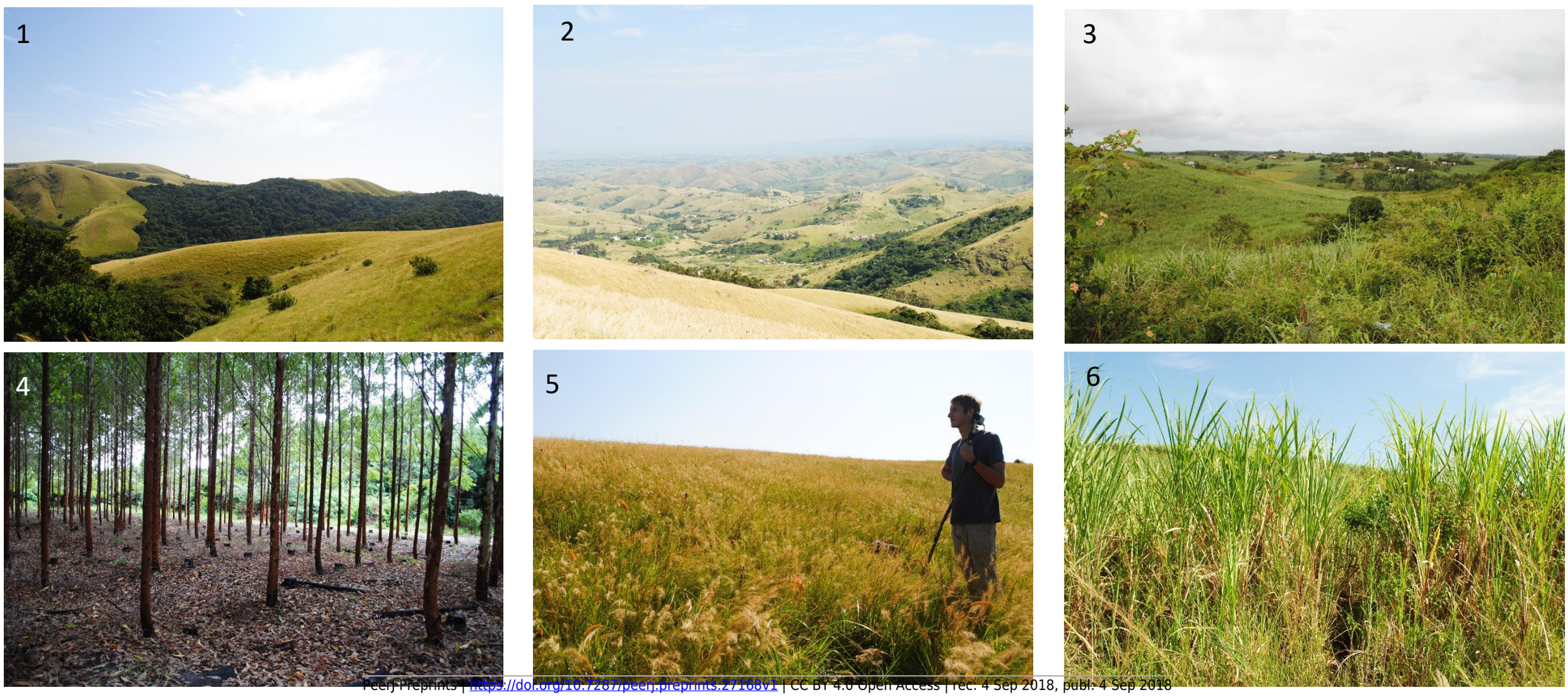

Table 1 (on next page)

Processing steps involved when analysing NDVI and thermal imagery

RED – Red reflectance values. NIR – Near-Infrared reflectance values.

PeerJ Preprints | https://doi.org/10.7287/peerj.preprints.27168v1 | CC BY 4.0 Open Access | rec: 4 Sep 2018, publ: 4 Sep 2018

1

Metric	Processing steps
$NDVI_{up}$	1. Read *jpg image, which consists of three bands 2. Extract band 1 (RED) and band 3 (NIR) 3. Compute NDVI as (NIR-RED)/(NIR+RED) 4. Compute statistics: mean, median, minimum, maximum and standard deviation
$NDVI_{down}$	1. Read *jpg image, which consists of three bands 2. Extract band 1 (RED) and band 3 (NIR) 3. Compute NDVI as (NIR-RED)/(NIR+RED) 4. Delineate region of interest in image (subset) using the clearly visible boundary 5. Compute statistics for subset: mean, median, minimum, maximum, number of pixels, and standard deviation
$Thermal_{ground}$	1. Read *csv file and plot as matrix 2. Delineate region of interest on the displayed file using the clearly visible boundary using the same extent of 150 x 150 cells 3. Compute statistics for each subset: mean, median, minimum, maximum, number of values and standard deviation

2

3

Table 2 (on next page)

Final models used to predict canopy attributes from Landsat spectral reflectance data and derived spectral and texture indices based on N = 115 data points.

Random forest models were computed with importance computation set to true and specifying 2000 trees (models converged after 791 trees for predicting *LAI* and 128 trees for *FCover*). Predictor variables include: mean of shortwave- infrared (SWIRM) and near-infrared (NIRM) reflectances, dissimilarity of near-infrared (NIRD) and of shortwave- infrared reflectances (SWIRD), and the mean of NDVI within a focal moving window of 8 pixels (NDVIMFocal). Predictor variables and their importance (with standard error in brackets) to the model predictions were ranked using the mean decrease in accuracy (%IncMSE) estimated based on random permutations using out-of-bag-Cross-Validation.

1

	LAI		**FCover**	
Final random forest model predictors	SWIRM+NIRM+NIRD+ SWIRD+ NDVIMFocal		SWIRM+NIRM+NIRD+ SWIRD+ NDVIMFocal+SD	
Variance explained	**34 %**		**30 %**	
Importance	NIRD	0.2954 (0.008)	NDVIMFocal	73.905 (1.975)
	NDVIMFocal	0.2718 (0.011)	NDVISD	45.443 (1.585)
	NIRM	0.2132 (0.009)	SWIRM	41.666 (1.569)
	SWIRD	0.1542 (0.009)	NIRD	39.588 (1.631)
	SWIRM	0.1291 (0.007)	NIRM	31.764 (1.753)

2
3

Table 3 (on next page)

Estimates of coefficients (a) and adjusted R^2 values (b) for relationships between habitat quality attributes at scale of sample points.

Mean/Median/Min and Max - Mean/median, minimum and maximum value of attribute estimated from the respective sensor's image at each sample point. Sample size varied for comparisons between variables: N = 108 ($NDVI_{down}$ vs $NDVI_{up}$), N = 138 ($NDVI_{down}$ vs $Thermal_{ground}$ and $NDVI_{up}$ vs $Thermal_{ground}$), N = 109 (*FCover* vs $NDVI_{down}$) and N = 139 (*FCover* vs $NDVI_{up}$ and *FCover* vs $Thermal_{ground}$). *LAI* estimates were only available at plot level and were thus excluded from this sample point scale analysis. Bold & grey shade: significance of estimate at $P < 0.001$; bold: $P < 0.01$; ns – not significant.

1

(a)		$NDVI_{down}$				$NDVI_{up}$				$Thermal_{ground}$			
		Mean	**Med**	**Max**	**Min**	**Mean**	**Med**	**Max**	**Min**	**Mean**	**Med**	**Max**	**Min**
NDVI down	**Med**	**0.99**											
	Max	ns	ns										
	Min	ns	ns	ns									
NDVI up	**Mean**	**0.51**	**0.47**	ns	ns								
	Med	**0.64**	**0.62**	ns	ns	**0.84**							
	Max	ns	ns	ns	ns	0.07	0.06						
	Min	**0.16**	**0.16**	ns	ns	ns	ns	**-0.70**					
Thermal ground	**Mean**	**3.53**	**3.26**	ns	ns	ns	ns	**-4.96**	**3.91**				
	Med	**3.51**	**3.22**	ns	ns	ns	ns	**-5.00**	**3.88**	**1.00**			
	Max	**4.47**	**4.31**	ns	ns	ns	ns	**-7.15**	**4.66**	**1.47**	**1.47**		
	Min	**3.23**	**2.99**	ns	ns	ns	ns	ns	**3.66**	**0.76**	**0.76**	**0.45**	
FCover		**-21.17**	**-22.7**	ns	ns	**19.31**	13.43	**101.4**	**-91.13**	**-4.13**	**-4.08**	**-2.56**	**-4.67**

2

(b)		$NDVI_{down}$				$NDVI_{up}$				$Thermal_{ground}$			
		Mean	**Med**	**Max**	**Min**	**Mean**	**Med**	**Max**	**Min**	**Mean**	**Med**	**Max**	**Min**
NDVI down	**Med**	**0.92**											
	Max	ns	ns										
	Min	ns	ns	ns									
NDVI up	**Mean**	**0.30**	**0.28**	ns	ns								
	Med	**0.39**	**0.39**	ns	ns	**0.82**							
	Max	ns	ns	ns	ns	0.04	0.03						
	Min	**0.08**	**0.09**	ns	ns	ns	ns	**0.23**					
Thermal ground	**Mean**	**0.17**	**0.15**	ns	ns	ns	ns	**0.05**	**0.07**				
	Med	**0.17**	**0.15**	ns	ns	ns	ns	**0.05**	**0.07**	**1.00**			
	Max	**0.11**	**0.11**	ns	ns	ns	ns	**0.06**	**0.06**	**0.92**	**0.92**		
	Min	**0.23**	**0.21**	ns	ns	ns	ns	ns	**0.08**	**0.93**	**0.93**	**0.78**	
FCover		**0.06**	**0.07**	ns	ns	**0.04**	0.02	**0.17**	**0.29**	**0.09**	**0.09**	**0.06**	**0.09**

3
4